



Water temperature of Alpine streams in response to discharge and radiation

By

George Charles Pea

A thesis submitted for the degree of Master of Science

School of Environment and Life Sciences
University of Salford
UK

October 2017

Abstract

The aim of this study is to examine the relationships between water temperature, discharge and their response to shortwave radiation in a highly glacierised Alpine basin. Due to the high altitude, the Alps have one of the highest solar radiation budgets in Europe and demonstrated almost double the rate of warming of the Northern Hemisphere. Understanding the effect radiation has on stream temperature is key as this is the primary control on water quality due to its influence on chemical, biological and physical processes. Studies of the Aletschgletscher basin have highlighted a paradoxical relationship between water temperature and air temperature; however there is limited research on the relationship between water temperature and solar radiation, which is of importance as radiation is the primary energy input (up to 80%) to Alpine proglacial streams. The river Massa in Canton Valais, Switzerland is the study areas, where the highly glacierised basin (65.9%) from which the rivers are sourced has shown high sensitivity to climatic warming. This is evident as Aletschgletscher has been recorded (2003) to be retreating by 20m a year. Hydrological data acquired from FOEN and shortwave radiation from Zermatt were analysed at high and low resolutions for the spring, summer and autumn. As expected seasonal runoff and radiation trends correlate with a lag time of up to 6 weeks between their peaks (2012), and water temperature has shown the paradoxical trend in summer; when radiation is at its highest levels water temperature decreases. This corresponds with the early ablation period when levels of discharge begin to increase, extending the cool tongue of water. During the ablation season water temperature has the highest range and undergoes periods of warm surges though radiation is still low. Stream temperature decreases from its peak at a high rate as discharge increases from the winter minima of approximately $0.5 \text{ m}^3\text{s}^{-1}$ to $3.5 \text{ m}^3\text{s}^{-1}$. While flow level is relatively low it proves to be the tipping point and demonstrates how radiation has a positive correlation with water temperature in spring but a negative correlation in summer due to the

increased runoff. The years 2003-2012 have shown water temperatures to peak between 1 April and 12 May, up to 2 months prior to radiation peaks. The implications of these findings are that water quality will deteriorate as stream flow decreases.

Contents

Abstract	i
List of tables	iv
List of figures	v
Acknowledgements	ix
Declaration	x
1 Introduction	1
1.1 Background	1
1.2 Climate change in the Alps	3
1.3 Glacier albedo	5
1.3.1 Stream albedo	5
1.4 Biological processes	6
1.5 Chemical Processes	7
1.6 Aim	8
1.7 Thesis outline	9
2 Controls on stream temperature	10
2.1 Introduction	10
2.2 Stream temperature and flow regimes	10
2.3 Energy inputs	14
2.4 Predicting stream temperature	15
2.5 Morphology of glacial rivers	16
2.6 Overview	17
2.7 Hypotheses and objectives	17
3 Methodology	19
3.1 Introduction	19

3.2	Selection of study area	19
3.3	Data acquisition	21
3.4	Data analysis	22
4	Results	23
4.1	Annual trends	23
4.2	Diurnal variation	43
5	Discussion	50
5.1	Seasonal trends	50
5.2	Diurnal trends	54
5.3	Stream morphology and topography	55
5.4	Future implications	56
6	Conclusion	61
6.1	Future regimes and further research	62
	References	63

List of Tables

3.1	Basin characteristics of the chosen study area, basin area (%) and basin glaciated (%).	20
4.1	Mean radiation (W m^{-2}) in Zermatt for the period 2003-2012.	24
4.2	Monthly percentage of total radiation and discharge for the year 2012.	24
4.3	Statistics of hourly discharge (m^3s^{-1}) of Massa for the period 2003-2012.	25
4.4	Statistics of hourly water temperature ($^{\circ}\text{C}$) of Massa for the period 2003-2012. The minimum temperature has not been included due all the observed years experiencing minima of 0°C	26
4.5	Monthly minimum, maximum, range and standard deviation of water temperature ($^{\circ}\text{C}$) for the months March- October 2012.	34
4.6	Annual total discharge (10^6 m^3) for the years 2003-2012 and the daily total of discharge from the day at which water temperature begins to decrease from the annual peak. With the percentage of the annual total added.	38
4.7	Total discharge (10^6m^3) from the January 1 up until the day water temperature decreases and the percentage of the annual total.	39

List of Figures

1.1	Retreat of Gornergletscher. Bottom image 1880s, top 2014 (source: World View of Global Warming, 2015).	2
1.2	Annual temperature anomalies ($^{\circ}\text{C}$) between 1901 and 2004 in Switzerland and the Northern Hemisphere (Rebetez and Reinhard, 2008).	4
1.3	Annual Swiss Alps mean air temperatures ($^{\circ}\text{C}$) for the period 1900-2003 (Zemp <i>et al.</i> , 2006).	4
1.4	Relationship between discharge (m^3s^{-1}) and albedo (α) in a proglacial stream draining from Place Glacier, Canada (Han, 1997).	6
1.5	Relationship between electrical conductivity ($\mu\text{S}/\text{cm}$) and discharge (m^3s^{-1}) in a proglacial Alpine stream (Dzikowski and Jobard, 2012).	8
2.1	Development of subglacial drainage system (a) May-June, (b) July and (c) August-September (Brown, 2002).	12
2.2	Average diurnal runoff (mm h^{-1}) curves for 5 months of a glacial river in the Austrian Alps (Milner & Petts, 1994).	13
2.3	Factors controlling stream temperature, black arrows representing associations with water exchanges (Moore <i>et al.</i> , 2005).	15
3.1	Map of Switzerland with Aletschgletscher basin and gauging locations. Zermatt also shown (Collins & Taylor, 1990).	21
4.1	Seasonal variation of discharge (m^3s^{-1}) as the black series and water temperature ($^{\circ}\text{C}$) as the blue series of the Massa for the years 2003 (a) to 2012 (j).	32
4.2	Seven day average of Massa water temperature ($\times 20$ $^{\circ}\text{C}$) in blue, Zermatt radiation (W m^{-2}) in red and discharge (m^3s^{-1}) in black of the year 2012 with the dashed line representing the summer solstice.	33

4.3	Daily average of hourly water temperature ($^{\circ}\text{C}$) in blue and discharge (m^3s^{-1}) in black for the Massa between the Julian days 91 and 152, 2012.	35
4.4	Daily average of hourly shortwave radiation (W m^{-2}) with lines added to highlight the increase of radiation over the period between the Julian days 91 and 152, 2012.	36
4.5	Daily average of hourly water temperature ($^{\circ}\text{C}$) in blue and discharge (m^3s^{-1}) in black between the Julian days 91 and 152, 2003-2012.	37
4.6	Daily average of hourly shortwave radiation (W m^{-2}) between the Julian days 91 and 152, 2003-2012.	38
4.7	Hourly variations of discharge (m^3s^{-1}) (black) and water temperature ($^{\circ}\text{C}$) (blue) between the Julian days 285 and 298, 2012.	40
4.8	Hourly variations of radiation (W m^2) (red) and water temperature ($^{\circ}\text{C}$) (blue) between the Julian days 110 and 117, 2012.	41
4.9	Hourly variations of radiation (W m^2) (red) and water temperature ($^{\circ}\text{C}$) (blue) between the Julian days 150 and 158, 2012.	42
4.10	Hourly variations of discharge (m^3s^{-1}) between the Julian days 110 and 117, 2012.	42
4.11	Hourly variations of discharge (m^3s^{-1}) between the Julian days 150 and 158, 2012.	43
4.12	Hysteresis plots of the hourly diurnal variation of water temperature ($^{\circ}\text{C}$) and discharge (m^3s^{-1}). Each graph at weekly intervals between the dates 14 May and 4 June 2012. 14 May (A), 21 May (B), 28 May (C) and 4 June (D).	45
4.13	Diurnal variation of water temperature ($^{\circ}\text{C}$), discharge (m^3s^{-1}) and shortwave radiation (W m^{-2}), for 26 April 2012.	47
4.14	Hysteresis plots of shortwave radiation (W m^2) and water temperature ($^{\circ}\text{C}$) for the dates 26/04/2012 (a) and 03/07/2012 (b). Key times and arrows added to indicate temporal variation.	48
4.15	Hysteresis plot of diurnal variation of water temperature ($^{\circ}\text{C}$) and discharge (m^3s^{-1}) for 14 May 2012 of the Massa, with the direction of the series represented by the arrows.	49
5.1	Schematic representation of monthly variations of water temperature, discharge and radiation. With the point of the summer solstice added.	53

5.2	Plot of the hourly discharge (m^3s^{-1}) and water temperature ($^{\circ}\text{C}$) for Massa 2012.	54
5.3	Satellite image of the upper reach of Massa demonstrating areas of topographical shading 04/10/2009 (GoogleEarth, 2017).	56
5.4	Annual mean temperature ($^{\circ}\text{C}$) in Switzerland from 1864 to 2015. Shown are the mean values of the individual years (black) and the smoothed curve (red) (Meteosuisse, 2016).	57
5.5	Schematic diagram of the transient snowline movement determining the proportion of the basin that receives snowfall or rain (Collins, 1998).	58
5.6	Schematic diagram of the relationships between energy input, water temperature and discharge in a river draining from an Alpine glacier (Collins, 2009).	59
5.7	Thought experiment to show how temperature increases through time coupled with declining ice area might first increase and then reduce discharge from the ice-covered area of a basin (Collins <i>et al.</i> , 2013).	60

Acknowledgements

Firstly I wish to express my deepest gratitude to the late Professor David N. Collins whom without it would not have been possible to complete my studies. His enthusiasm and dedication to the study of Alpine environments is what motivated me to remain at the University of Salford and continue my studies under his guidance. I am forever thankful for the memories and friendship shared with David.

Also I'd like to thank my supervisor Dr Neil Entwistle for his assistance in helping the completion of my research and also the contribution to many memorable trips. Many thanks also to Dr Rob Williamson and my fellow post-graduate Kirk Larsen for having the time and patience to assist me and offer guidance throughout my time as a student. Finally I'm thankful for the support from my family and friends throughout these two challenging years.

Declaration

This is to certify that the copy of my thesis, which I have presented for consideration for my postgraduate degree embodies the results of my own course of research, has been composed by myself and has been seen by my supervisor before presentation.

Signature

Date

1

Introduction

1.1 Background

Air temperature in the European Alps has risen by a mean annual total of 2 °C during the 20th century, which is approximately twice the warming rate of the northern hemisphere annual average (Gobiet *et al.*, 2014). The primary impact of this increased warming is the retreat of Alpine glaciers; an estimated 50% of the original glacier volume has vanished since the end of the Little Ice Age in 1850 (Wegmann *et al.*, 1998). This is of great concern as more than one-sixth of world's population rely on glaciers/ seasonal snow packs for their fresh water supply (Barnett *et al.*, 2005). Figure 1.1 shows an example of the extent to which Alpine glaciers have retreated between the 1880s and the present decade. The particular glacier in the example is Gornergletscher.

Knowledge concerning the impacts of climate change on Alpine hydrology and the dynamics of proglacial streams is key to the understanding of water quality and future implications of glacial retreat. High mountainous streams are ideal study areas for the effects of climate change on water quality due to these systems having little to no human interference and reflect an almost complete natural river system. Water temperature is a major factor of stream quality. Numerous physical, chemical and biological processes in aquatic systems are driven by temperature (Brown and Hannah, 2008). Stream temperature has a major control on aquatic habitat due to its influence on species distributions, dissolved oxygen concentrations and the growth and also the development rate of organisms (Webb *et al.*, 2008). Hari *et al.*, (2006) found a strong correlation between the increase of water and air tem-



Figure 1.1: Retreat of Gornergletscher. Bottom image 1880s, top 2014 (source: World View of Global Warming, 2015).

perature in Alpine basins and the sharp decline of brown trout populations in Western European streams. Findings such as these show how crucial water temperature is on the quality of aquatic habitats. As well as a major water quality parameter, stream temperature is also a key indicator of the water source as each has specific thermal characteristics (Brown *et al.*, 2006). Irrespective of discharge, meltwater exits the glacier around 1°C ; however, warming downstream is driven by energy input and flow. Proglacial streams have displayed fast responses to meteorological forcing making water susceptible to changes downstream (Magnusson *et al.*, 2012) and radiation fluxes account for more than 70% of heat input. With the exception of shaded streams radiation is the primary driver of summer water temperature variability and therefore stream albedo has the potential to be a significant influence on heat inputs. Shortwave radiation increases with altitude due to the reduction of clouds, ozone, aerosols and air molecules and as a result the Alps possess one of the highest UV radiation levels in Europe (Schmucki and Philipona, 2002).

Albedo is the reflectance of a surface, and in water it is known to vary with turbidity, aeration, suspended sediment concentration, algae and the roughness of stream surface (Cogley, 1979; Webb *et al.*, 2008). However it is largely dependent on the angle of radiation input. Albedo of water is therefore a function of latitude (Cogley, 1979). Leach and Moore (2010) measured albedo of a low gradient stream between 0.05 and 0.1; however the type of mountain stream focused in this thesis are of higher gradient and

flow in bouldered channels where water becomes increasingly aerated.

1.2 Climate change in the Alps

The Alps are highly sensitive to climatic warming in comparison to the rest of the Northern Hemisphere. Figure 2.1 compares the annual temperature anomalies in Switzerland and the northern hemisphere between 1901- 2004. Monthly mean temperatures were gathered from 12 weather stations in Switzerland and then homogenised (Rebetez and Reinhard, 2008). From 1980 there is a clear period of enhanced warming in both data sets however the Swiss series has an accelerated rate of increase. Gehrig-Fasel *et al.*, (2007) highlighted this accelerated warming through the analysis of measurements from 24 MeteoSuisse weather stations situated between 1650-2450m, Figure 2.2 shows the annual mean temperatures ($^{\circ}\text{C}$) steadily increasing from 1900 through to 2003 the bold black line representing the 10 year mean. There are a variety of fluctuations during this period with a general pause from 1960-1980 before there is a steep increase. This thesis focuses on measurements acquired only between 2003-2012, this period is too short to display any long time temperature changes.

Air temperature and precipitation are the two greatest climatic factors influencing the health of a glacier (Zemp *et al.*, 2006). The scenario presented by Zemp *et al.*, (2006) predicts Alpine glaciers to completely disappear within decades as much of the ice is located below 3000m a.s.l. Negative glacier mass-balance in the Alps is resulting in a reduction of glacier and snow-melt contributing to Alpine streams with groundwater becoming a major source (Brown *et al.*, 2007). This shift in water sourcing has a significant effect on the water chemistry and biology as groundwater is solute rich and has a higher temperature in comparison to snow and ice melt water.

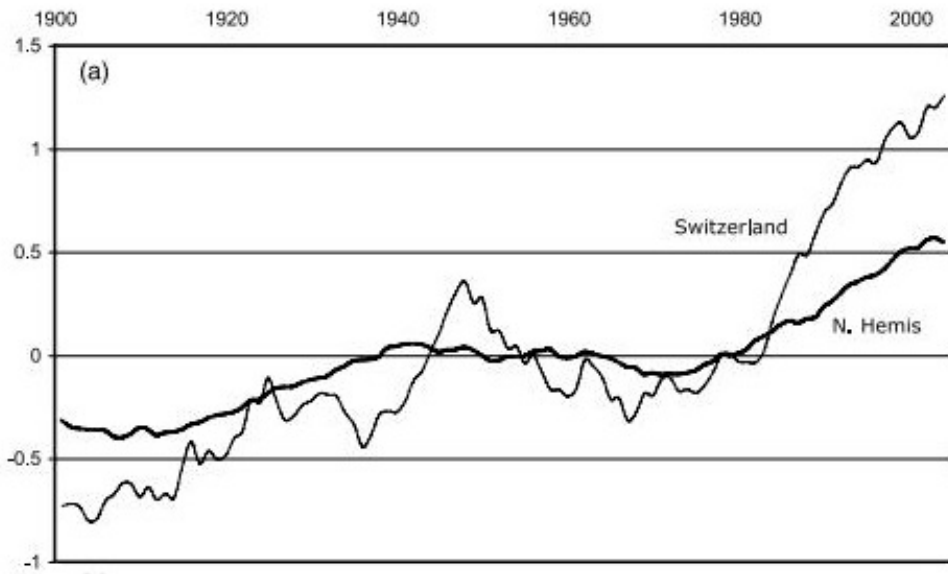


Figure 1.2: Annual temperature anomalies ($^{\circ}\text{C}$) between 1901 and 2004 in Switzerland and the Northern Hemisphere (Rebetez and Reinhard, 2008).

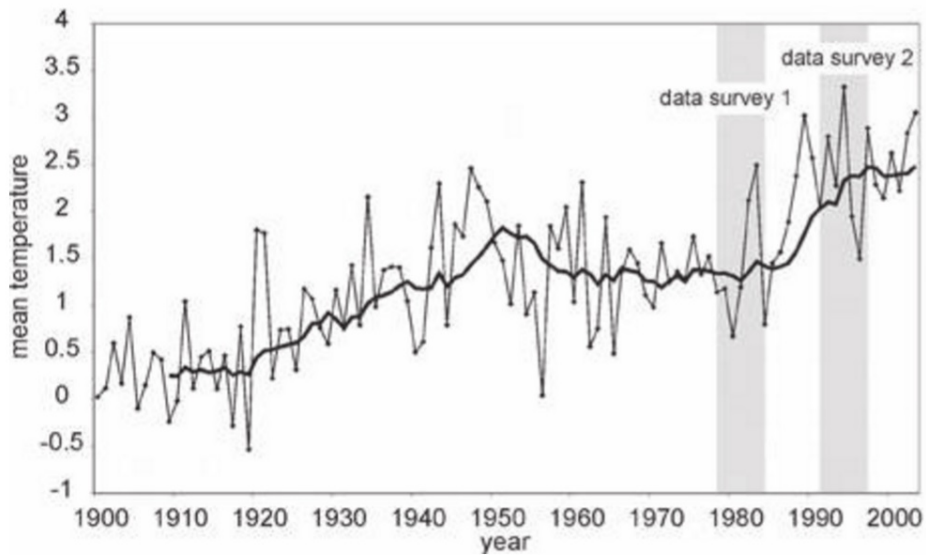


Figure 1.3: Annual Swiss Alps mean air temperatures ($^{\circ}\text{C}$) for the period 1900-2003 (Zemp *et al.*, 2006).

1.3 Glacier albedo

Climatic warming in the Swiss Alps has resulted in a decrease of snow days (Ceppi *et al.*, 2012; Marty, 2008; Scherrer *et al.*, 2004). The amount of snowfall in the winter months determines the temperature and duration of the following spring and summer due to the SAF effect. Surface albedo within the basin increases with a higher amount of snowfall. If the previous winter was mild, experiencing reduced snowfall, water temperatures are expected to be lower in the following months. This occurs as the ablation season will begin earlier due to less snow reflecting incoming radiation and increasing the rate of glacier ice melt. Furthermore the higher and sooner the transient snowline rises the longer and larger area of ice and snow there is to melt therefore increasing runoff. Additionally as the snowline elevation increases the greater the area in which precipitation falls as rainfall increases (Collins, 1998; 2009).

1.3.1 Stream albedo

Richards and Moore (2011) addressed the dependence of stream albedo on discharge at a study site downstream of Place Glacier, Canada in a relatively low gradient step pool in a boulder dominated channel. A positive correlation between discharge and albedo was found (Figure 1.4) during this study period. This was consistent with the study hypothesis of increasing aeration influencing the albedo of the water surface. Stream surface albedo increased from around 0.1 (10% reflected) at lower flows to 0.4 (40% reflected) at higher flows. Due to Alpine glaciers retreating, discharge will soon reach a tipping point and begin to decrease due to reduced glacial mass. Therefore bearing these findings in mind albedo will begin to decrease and water temperatures will rise. However the effect of suspended sediment and its role on albedo has not been addressed, which could be of importance as suspended sediment has demonstrated to increase water albedo further (Han, 1997).

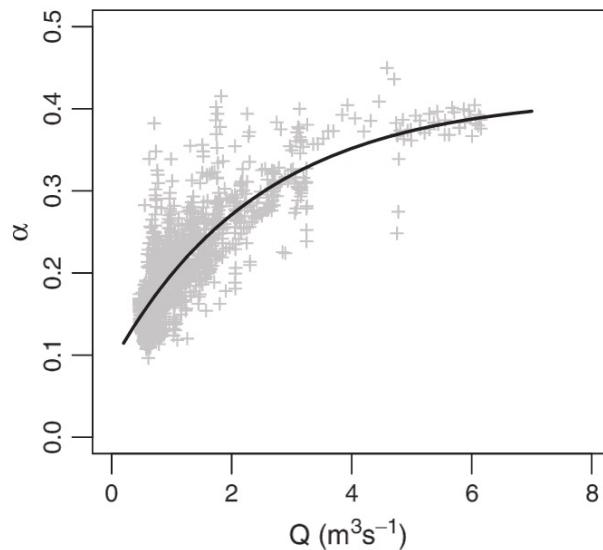


Figure 1.4: Relationship between discharge (m^3s^{-1}) and albedo (α) in a proglacial stream draining from Place Glacier, Canada (Han, 1997).

1.4 Biological processes

Proglacial streams are a severe environment highly characterised by the sediment load and water temperature. Steffan (1971) outlined that habitats in rivers sourced from glaciers are considerably different from other fresh water habitats and he therefore placed them in a distinct biotope termed kryal. Water temperature has the influence to render the river catchment a suitable habitat for native species. The control temperature has on biological processes is immense, as it directly influences physiology, metabolic rates of aquatic species and the nutrient cycle process (Fisher, 1995). As previously discussed in section 1.1, there has been a noticeable correlation between the catchment of brown trout in Western European Alpine rivers and rising air temperatures in the late 20th century. Hari *et al.*, (2006) discussed that due to water temperatures increasing, brown trout have declined as habitats are being pushed upstream to cooler climates; however this movement has been blocked by typical Swiss Alpine streams on average possessing 1-2 vertical barriers with drops of 15cm or more every 100m. This loss of habitat is a major contribution to their population decline and displays the fragile nature of aquatic habitats when water temperature changes (Hari *et al.*, 2006).

In terms of biota in proglacial streams these are mainly in the form of micro-

organisms such as bacteria dominated biofilms (Battin *et al.*, 2001; Rott *et al.*, 2006). These aquatic lifeforms also have a specific range of temperature that they can survive and so any change in this can restrict their habitat. Alpine proglacial stream discharge levels are directly influenced by the meteorological conditions, therefore with climate change the river thermal patterns will be altered affecting the sensitive biota (Poole and Berman, 2001). It is expected that with the retreat of glaciers in the long term, stream temperatures will increase the composition of particles in the stream and the nutrient cycle rate (Milner *et al.*, 2010).

1.5 Chemical Processes

Proglacial streams have three principal water sources with their own chemical and thermal characteristics. These sources include precipitation, ice/snow melt and groundwater. Glacier fed streams have high levels of suspended sediment and solutes. Solute in the runoff is acquired from the atmosphere in the form of precipitation, dry deposition and from chemical weathering of subglacial and ice marginal rock (Bundi, 2009). Such reactions include sulphide oxidation and carbonation (Brown *et al.*, 1994). Electrical conductivity is an efficient method of establishing the solute concentration of rivers, thus the system from which the particular discharge has originated. Discharge sourcing from groundwater flow has a higher temperature than glacier melt and is solute rich due to an increased residence time with the underlying geology (Singh and Hasnain, 2002). Snow-packs influence Alpine river basins to a high extent by controlling peak stream discharge in the early summer due to retainment of meltwater in the ablation zone. Runoff resulting from snow-pack melt has a generally low level of suspended sediment and a low temperature. In contrast glacier/ ice melt hosts a large level of sediment yields which have been flushed out from newly exposed subglacial sediment (Bundi, 2009). The final source for Alpine proglacial streams is precipitation. The chemical characteristics of this include a poor solute level and a high temperature.

Negative correlation exists between electrical conductivity and discharge, as discharge increases solute concentration/ electrical conductivity decreases due to a higher volume of water diluting the solutes. Furthermore Collins (1979) explained this inverse relationship exists due to solute enriched groundwater being mixed with relatively solute free supraglacial water (see Figure 1.5). As discussed groundwater has a higher temperature and solute

concentration than snow and ice melt. Understanding water sources of Alpine streams and rivers is key especially in regions such as Switzerland that depend on hydropower for much of their energy. High solute concentration can affect these dam systems by eroding components such as turbines and depositing sediment, disrupting the mechanical processes of the dams. Williams *et al.*, (2016) expressed the importance of understanding the solute concentration of rivers through models so as to predict the extent of erosion in the hydroelectricity dam component. This knowledge is critical when determining whether a catchment is viable for an efficient hydroelectricity scheme or not.

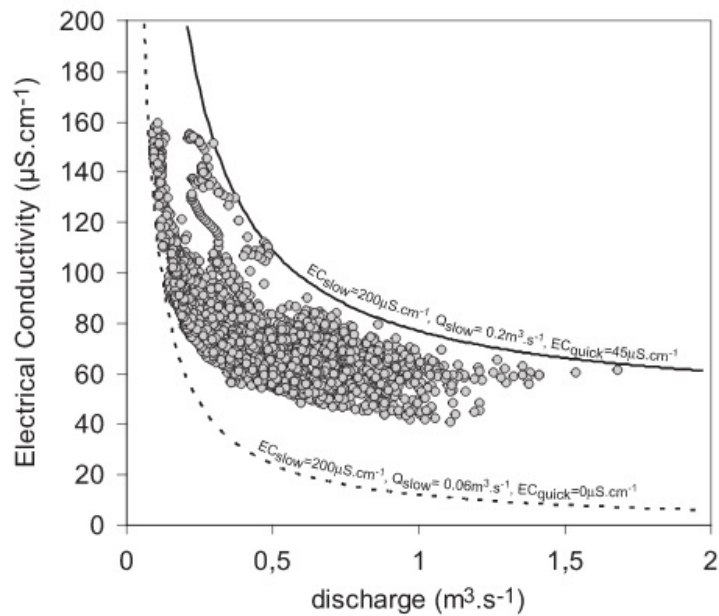


Figure 1.5: Relationship between electrical conductivity ($\mu\text{S}/\text{cm}$) and discharge (m^3s^{-1}) in a proglacial Alpine stream (Dzikowski and Jobard, 2012).

1.6 Aim

The aim of this study is to determine the dominant controls currently operating on water temperature in streams emerging from glaciers with a view to predicting how such controls may change in a warming climate.

1.7 Thesis outline

This thesis is over six chapters. Chapter 1 comprises seven sections, the primary focus of the chapter is the introduction and background of the current understanding. The chapter concludes by outlining the aim and hypotheses of the thesis.

Chapter 2 encompasses the controls on stream temperature in five sections also including a section as an overview and highlights research gaps. Chapter 2 concludes with the objectives and hypotheses. Chapter 3 discusses the method of acquiring the data used in the results and also the justification of the chosen study area. The results are presented in Chapter 4 and are organised in two sections; Annual trends and Diurnal variation. Chapter 5 the Discussion outlines the key findings of the results and their importance. This chapter is organised into four sections; Seasonal trends, Diurnal trends, Stream morphology and topography and finally Future implications. To conclude the thesis chapter 6 discusses whether the aims and objectives outlined were achieved and suggests future implications.

2

Controls on stream temperature

2.1 Introduction

This chapter will address the controls on stream temperature and the typical thermal and flow regimes of an Alpine proglacial stream using research from previous studies. There are numerous factors that control stream temperature including albedo, meteorological parameters, stream morphology, level of discharge and water source. Flow regimes in glacierised basins are strongly controlled by the glacier therefore the process of the drainage system of Alpine glaciers has been explored.

2.2 Stream temperature and flow regimes

Stream temperature is a primary water quality parameter but the study of interaction between stream temperature and flow is limited (Constantz, 1998). In the Alps climate change is the main factor affecting water quality but not the only factor with land use evolution, deforestation and other human activities also contributing to the degradation of water quality (Delpla *et al.*, 2009). Meltwater exits Aletschgletscher at around 1 °C irrespective of flow, which creates a tongue of cold water extending from the glacier; as the water flows across the proglacial basin it is heated and continues to warm further downstream. Alpine proglacial stream temperature varies diurnally and seasonally due to numerous natural variables including air temperature,

precipitation, groundwater exchanges, discharge and solar radiation. Alpine proglacial streams often possess stretches of water with large surface area to volume ratios and therefore reflect high diurnal variations in stream temperature due to greater rate of penetration from solar radiation (Constantz, 1998). Large seasonal variations in stream temperature are also to be expected due to the wide range of solar radiation and air temperature regimes that Alpine environments possess.

Flow regimes in glacierised catchments are strongly controlled by the glacier mass balance when basins are 20%+ glaciated. The generation of discharge from snow and ice melt generally is inverse to flow regimes of temperate fluvial environments as maximum flow occurs in summer when precipitation is lowest (Brown, 2002; Fountain and Tangborn, 1985). The volume of water in the proglacial stream determines the length of time available for heat exchanges as a higher volume of water increases velocity, which would therefore reduce interaction time a parcel of water has with the surrounding environment (Brown *et al.*, 2006). There is a great variation of discharge seasonally with lower levels in the winter months due to glacier accumulation and precipitation in the form of snow in contrast to spring and summer with high discharge from the ablation period and precipitation falling as rain (Huss *et al.*, 2008). Groundwater possesses a higher temperature than meltwater and so increased groundwater contributions to Alpine streams result in higher water temperatures, particularly in the winter and early spring when meltwater contribution is low (Milner *et al.*, 2009).

In winter, precipitation in Alpine glaciated basins falls in the form of snow with temperatures only getting high enough in spring to melt the snow-packs and ice. Snow does not have any immediate positive effect on runoff but increases surface albedo of the glacier and the reattainment of water. Figure 2.1 shows the schematic representation of the seasonal development of subglacial drainage system in an Alpine glacier from the early melt season in May and June (a), (b) July and through to (c) August- September (Brown, 2002). As radiation and air temperatures increase in early spring the ablation period begins, discharge does not respond immediately to this increased rate of melt due to much of the water being withheld by ice and delayed by snow-packs, this lag time can extend into the summer months as water is often held within subglacial pockets and ice dammed lakes (Collins, 1984). The snow covered surface of the glacier in spring delays the melt water draining from the glacier and the conduit systems forming. In contrast precipitation during summer can have an immediate effect on runoff as there is little snow on the glacier and the subglacial drainage system has formed to efficiently release water from melt and rain. Rainfall on bare glacier ice

runs off almost immediately into the subglacial passages. Towards the end of summer, discharge decreases as the supply of subglacial and englacial water has been drained (Benn & Evans, 2014).

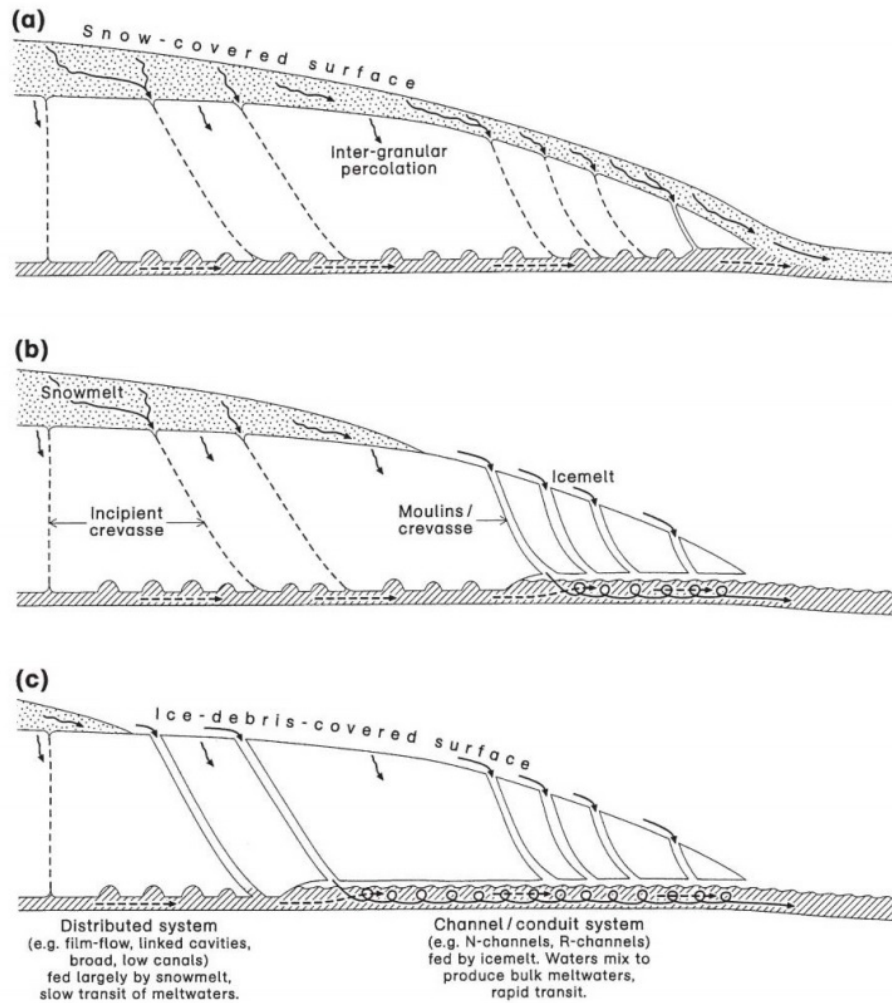


Figure 2.1: Development of subglacial drainage system (a) May-June, (b) July and (c) August-September (Brown, 2002).

The flow regime of Alpine proglacial streams also varies diurnally, particularly in the ablation season as the discharge responds greatly to air temperature and precipitation fluctuations (Fenn, 1985). The diurnal variation of glacial rivers in the melt season typically follows the regime of a late afternoon peak and a recession through the evening and night. Figure 2.2 shows the average 24 hour runoff (mm h^{-1}) curves over 5 months from a glacial river in the

Austrian Alps (Milner & Petts, 1994). This basin is 84% glaciated which is significantly higher than the basin selected for the area of study in this thesis; these curves display a clear transformation of runoff levels from May to August with little diurnal variation in May to a significant one in September. Daily discharge peaks often lag behind air temperature peaks by up to a few hours (in the later ablation season) due to the distance meltwater has to travel through the subglacial drainage system (shown in Figure 2.1). This lag time is extended in periods when the glacier is still covered with snow such as spring and the early months of summer as Figure 2.1(a) displays (Benn & Evans, 2014).

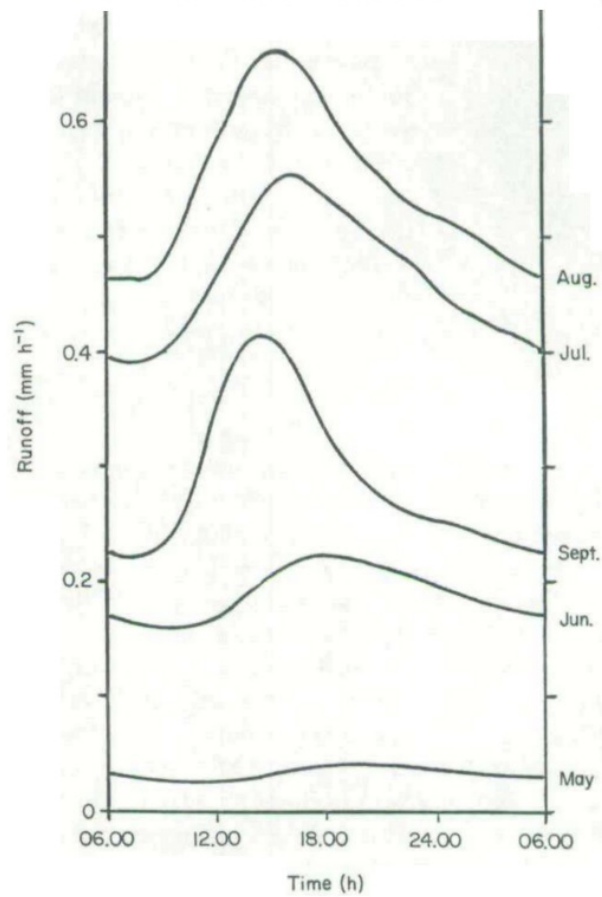


Figure 2.2: Average diurnal runoff (mm h^{-1}) curves for 5 months of a glacial river in the Austrian Alps (Milner & Petts, 1994).

2.3 Energy inputs

For many mountain glaciers shortwave radiation flux is the main energy input for ablation (Wagnon *et al.*, 1999). This is greater for glaciers that have been retreating for sometime with the exposure of side moraines which deposit dust and debris on the glacial ice reducing the surface albedo, which is the case with most glaciers in the Alps (Oerlemans *et al.*, 2009). Shortwave radiation drives the biological and physical processes at the earth's surface while atmospheric components (aerosols, CO₂, ozone, water vapour etc) interact with solar shortwave radiation by scattering or attenuating depending on the concentration of gas and particulate matter in the atmosphere; such interactions result in atmospheric heating or re-radiated energy in the form of longwave radiation. Shortwave radiation peaks at solar noon in contrast to longwave radiation which remains relatively constant (Lowney, 2000).

Recent studies on glacierised basins have revealed the complex thermal behaviour of proglacial streams (Brown *et al.*, 2006; Cadbury *et al.*, 2008; Webb *et al.*, 2008). Solar radiation is a crucial environmental factor in Alpine water due to the natural increase of ultraviolet radiation flux with elevation (Sommaruga, 2001). Figure 2.3 shows a schematic view of factors controlling stream temperature with the black arrows representing energy fluxes associated with water exchanges (Moore *et al.*, 2005). There is limited vegetation in the proglacial area to obstruct incoming solar radiation, then the only shading will be the topography or cloud cover. Topographical shading is a major influence on proglacial streams in the Alps due to the steep banks and narrow valleys that are typical in the region. Latitude also is a key factor influencing shading as Canton Valais is situated at 46.1905° latitude therefore the angle of the sun is fairly acute. Water exits the portal of Aletschgletscher at <1 °C (Collins, 2009), as the water flows downstream from the terminus through the proglacial field it is heated by solar radiation. Heat transfer within river systems is complex, additional energy exchanges that influence proglacial stream temperature include: channel friction, groundwater flow, condensation, evaporation, bed heat conduction and air temperature (Caisie, 2006).

Stream bed friction is also considered a primary energy source in proglacial streams, this process is most prevalent in high gradient streams, the Massa and Gornera for example (Chikita *et al.*, 2010). The surface area of the stream increases with discharge therefore bed friction is greater however the heat capacity of the stream has increased therefore friction remains at a steady level. A previous study at a proglacial stream fed by the Gulkan

Glacier, Alaska in the summer of 2006 resulted in net shortwave radiation and stream bed friction occupying *ca.*70% of the total thermal input to the stream (Chikita *et al.*, 2010).

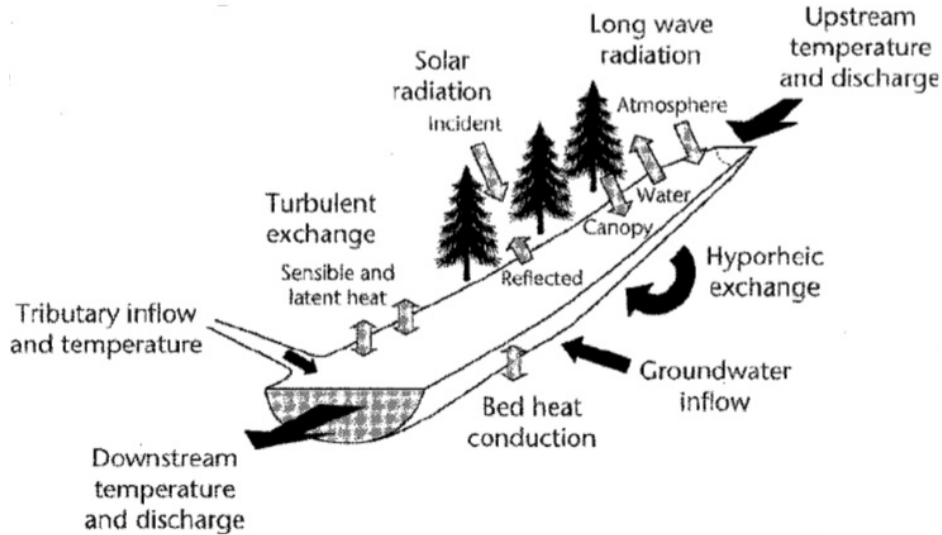


Figure 2.3: Factors controlling stream temperature, black arrows representing associations with water exchanges (Moore *et al.*, 2005).

2.4 Predicting stream temperature

The use of models that predict or simulate stream temperatures is becoming increasingly important. There are two categories of water temperature models; statistical and deterministic. Statistical models are relatively simple and require minimal data inputs while deterministic models require numerous input data such as depth and velocity (Benyahya *et al.*, 2007). An example of a simple energy balance equation is presented in Box 1 (Magnusson *et al.*, 2012). The equation describes the downstream change of temperature ΔT ($^{\circ}\text{C}$) over a stream reach length L (m) and average width w (m). Q (W m^{-2}) is the heat flux across the stream surface c ($\text{J kg}^{-1} \text{K}^{-1}$) the specific heat capacity of the water, p (kg m^{-3}) the water density. Δz (m) the change of altitude from upstream reaches to downstream, gravitational acceleration g (m s^{-2}), stream discharge as q (m^3s^{-1}) and residual temperature change as ΔT_r ($^{\circ}\text{C}$).

$$\Delta T(t) = \frac{Q(t)w(t)}{q(t)} \frac{L}{cp} + \frac{g\Delta z}{c} + \Delta T_r(t)$$

This equation predicts how temperature will change on a stream reach as a result of surface heat transfer and frictional heating. Surface heat exchange cools and warms the stream at a rate proportional to the heat flux, the length of the stream and average width, and inversely proportional to discharge (Magnusson *et al.*, 2012). Models predicting water temperature from glaciers with a negative mass balance are proving to be of greater importance as thermal and flow regimes are expected to be altered (Collins *et al.*, 2013).

2.5 Morphology of glacial rivers

Fluvial processes of glacier-fed streams are characterised heavily by morphology. Typically the proglacial stream channel is braided in the outwash plain due to the high sediment load flushed from the glacier and aggradation; these channels migrate laterally across the valley floor (Milner & Petts, 1994). Hickin (1993) suggests that fluvial hydrosystems of glacial rivers have three stages of progression:

1. Highly unstable, braided form, steeply graded and possesses a high width to depth ratio;
2. Wandering type with irregular sinuous, laterally mobile, often with secondary channels separated by vegetated islands;
3. Relatively stable with a meandering single channel, high sinuosity and a reduced width to depth ratio.

Each stage resembles a different thermal regime. The first stage possesses a high width to depth ratio reach, which will have a lower heat capacity and a larger surface area of water in contact to with the environment, so heating will occur at a high rate here in comparison with the other stages. Downstream vegetation increases, with this riparian shading reducing the direct contact with solar radiation and stream warming processes. Once the river forms a single channel the surface area will decrease and heat capacity increase reducing the rate of warming by meteorological parameters. Friction is

greater in wide shallow streams and less in narrower, deep streams. Therefore stream bed friction will be more dominant in stages 1 and 2 (Milner & Petts, 1994).

2.6 Overview

Previous studies expressed the complexities of proglacial streams and the basin's sensitivity to climatic warming (Cadbury *et al.*, 2008; Collins, 2009; Webb *et al.*, 2008). Shortwave radiation is the primary energy input of proglacial streams and is a controlling factor of runoff and water temperature however there is limited research on the diurnal and seasonal variation of water temperature; discharge and their responses to radiation fluctuations. Alpine glaciers are in a period of accelerated retreat in response to increasing air temperatures. Understanding the seasonal and annual thermal characteristics of Alpine proglacial streams is important. The Alps have displayed a significant response to climate change therefore the thermal regimes across the seasons and years are to be observed as the effects temperature has on the quality of water in terms of habitats and biota but also the dependency that the region has on glacial and snow-pack melt as a fresh water source for agriculture, industry, consumption and hydroelectric purposes.

2.7 Hypotheses and objectives

The objectives of the thesis are as follow;

1. To analyse the diurnal, seasonal and annual variations of stream temperature and discharge in a year of high recorded shortwave radiation levels.
2. To identify the level of flow in which stream temperature decreases.
3. To assess the control shortwave radiation has on stream temperature.
4. To understand why water temperature decreases in late spring and early summer when radiation peaks.

The hypotheses for the thesis are listed below.

1. Stream temperature is warmest in spring when discharge is low and shortwave radiation is high.

2. Discharge is the primary control on alpine stream temperature.
3. A paradoxical relationship exists between stream temperature and short-wave radiation.

3

Methodology

3.1 Introduction

The primary control of stream temperature will be identified through radiation, water temperature and discharge measurements. It would be expected that as solar radiation levels peak during the ablation season, water temperature would also peak. The ablation season shall be under close scrutiny in order to understand the transforming relationship between water temperature and discharge as radiation rises.

3.2 Selection of study area

The basin of the river Massa was selected for study. Table 3.1 displays the characteristics of this basin. This river is situated close to Zermatt, a town located in the Central Swiss Alps of the Canton of Valais at the southern end of the Matter Valley (MeteoSwiss). Zermatt is also the location in which shortwave radiation levels are recorded. The European Alps are one of the most intensively studied mountain ranges in the world (Haeberli & Beniston, 1998) and this region provides access to multiple weather and gauging stations which are situated at a variety of elevations with areas of permanent and seasonal snow cover. Decades of data are also available because of the continuous monitoring undertaken by numerous researchers. The Massa has been chosen as the Aletschgletscher is the most voluminous glacier in the Alps and is an indicator of long-term climate trends as it is not sensitive to short-term climate fluctuations in which smaller glaciers in

Table 3.1: Basin characteristics of the chosen study area, basin area (%) and basin glaciated (%).

River	Basin area (km²)	Basin glaciated (%)
Massa	195	65.9

the Alps have shown; such as the period of advance in the 1920s and 1980s (Jouvet *et al.*, 2011).

The climatic conditions in the Matter valley have a continental character with low precipitation and high-radiation budgets (Randin *et al.*, 2009). Average annual precipitation is only approximately 475 mm, which is one of the lowest in Switzerland. This low precipitation is due to the valley surrounded by high peaks that often exceed 4,000m a.s.l. in elevation (Hill, 2012). Canton Valais therefore is extremely reliant on glacial melt as a fresh water source thus studying the quality of this water and the forces controlling it is highly important.

The river Massa draining from Aletschgletscher is the primary focus of the study. Aletschgletscher is the largest glacier in the Alps with the basin measuring 195km², 65.9% of which is glaciated. The gauging station in which the water temperature and discharge measurements derive is situated 1458m a.s.l. (2.4km from the glacial portal), which is the lowest point of the basin that ranges up to Aletschhorn at 4194m a.s.l. The mean annual runoff (1957-2005) of the basin is 2.112m (Collins, 2008). The river is approximately 7km long and passes through the Massa gorge and onwards into the Rhone.

The basin areas (km²) and total glaciated area of the basin (%) for the study areas are shown in Table 1.1. Almost two thirds of Massa’s basin is glaciated and it is Alpine and high Alpine in character it is also classed as a hydrological research basin by the Swiss National Hydrological and Geological Survey and therefore human interference is minimal (Braun and Renner, 1992). Figure 3.1 display maps of the study basins and region with the gauging stations added.

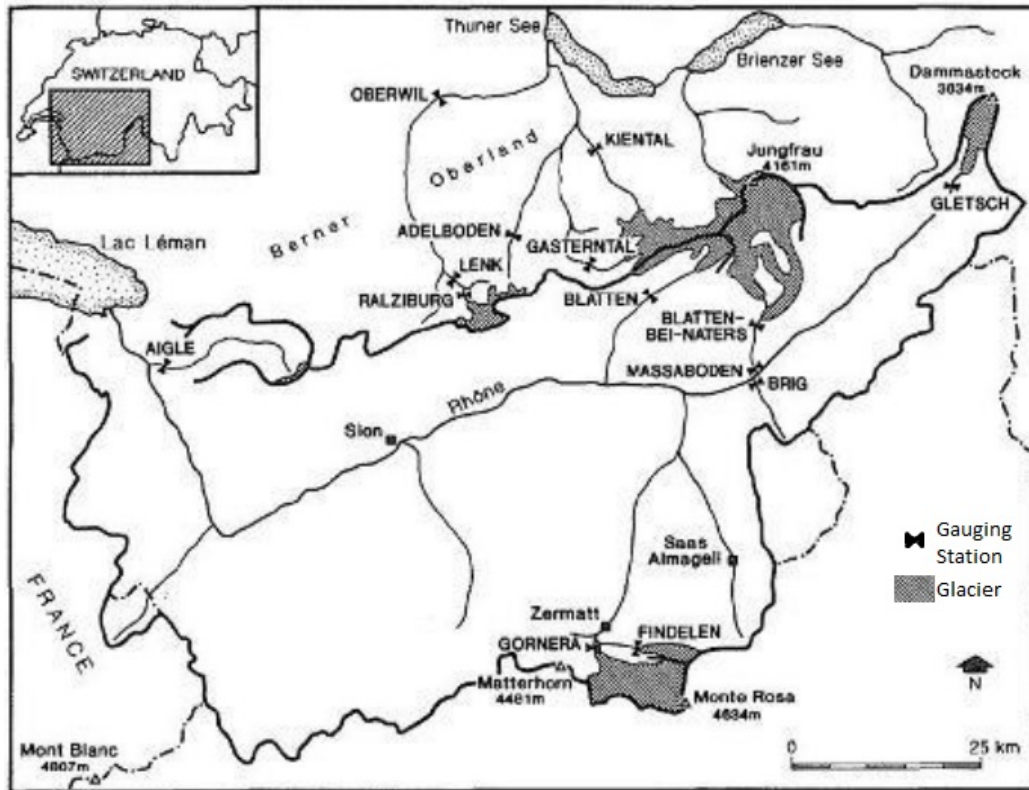


Figure 3.1: Map of Switzerland with Aletschgletscher basin and gauging locations. Zermatt also shown (Collins & Taylor, 1990).

3.3 Data acquisition

Hydrological data was gathered from the Swiss Federal Office of the Environment (FOEN); this method of data allows in depth analysis as it is at a high resolution and measurements are collected on the hour everyday for the whole year from a gauging station situated on the river. Local shortwave radiation data was not available at the Massa river site and therefore hourly measurements from Zermatt have been used. The possible implications of the unavailability of local shortwave radiation measurements to the Massa is that it will not express the true levels of radiation of the basin as the basin is situated at a higher altitude and approximately 45km away from Zermatt; however the radiation data will still show the temporal variations at a regional scale. Continuous hourly data is also available for the years 2003-2012 which allows precise comparisons and time series with water temperature

and discharge.

3.4 Data analysis

The years 2003-2012 are analysed since there are complete and continuous annual records of radiation, water temperature and discharge measurements. Hourly measurements of discharge at Massa were processed into annual data sets for the calendar years 2003-2012 by manually selecting and separating data recorded into different years. Annual trends are analysed by calculating the mean, maximum, minimum and standard deviation of water temperature and discharge in order to assess trends between the parameters. This method of analysis has been used by Brown *et al.*, (2006). Annual mean radiation will be analysed to signify the years with the highest and lowest totals. An objective is to analyse seasonal runoff and thermal regimes of the Massa, which is achieved by hydrographs of water temperature and discharge similar to those of Collins (2009); however both parameters are plotted on the same graph for a clearer illustration of potential relationships. The year 2012 is chosen to analyse seasonal, diurnal and daily measurements in depth as this is the most recent year with complete data available. Moreover previous studies have not analysed a year as recent as 2012. Seasonal radiation also is analysed, however this has high hourly fluctuations and therefore is processed into a series of weekly means so it can be compared with discharge and temperature.

Brown *et al.*, (2006) analyses hourly air temperature and water temperature over a weekly period, the same method of analysis is used in this thesis; however using shortwave radiation measurements not air temperature. This will contribute to the objective of understanding the diurnal and daily relationship between radiation and water temperature and also the control that radiation has on water temperature. To understand the level of flow at which stream temperatures cease to surge and decrease from the peak will be achieved by analysing the daily average water temperatures and outlining the point at which the decrease begins. This analysis will also contribute to the understanding why stream temperature decreases in late spring and early summer when radiation peaks.

4

Results

Annual, seasonal and diurnal analysis of radiation, discharge, water temperature from the Massa river are presented in this section.

4.1 Annual trends

The average annual radiation for the years 2003-2012 is shown in Table 4.1. 2012 has the highest average radiation with 2004 having the lowest. As 2012 has the highest average annual radiation for the recorded years and is the latest year with complete data it shall be the year chosen to have further analysis. The monthly percentage of the total annual radiation for 2012 is displayed in Table 4.2. May, June, July and August have the highest percentages, with the year having 50.11% of the years total radiation. June has the highest percentage of 13.05% and December with the lowest of 2.49%. It was expected that June would have the highest total radiation due to it being the month of the summer solstice (20 June). Seasonal radiation levels follow that of a typical mid-latitude region.

Table 4.1: Mean radiation (W m^{-2}) in Zermatt for the period 2003-2012.

Year	Mean
2003	162.45
2004	154.2
2005	157.75
2006	157.42
2007	158.7
2008	156.22
2009	164.19
2010	160.05
2011	161.78
2012	164.46

Table 4.2: Monthly percentage of total radiation and discharge for the year 2012.

Month	% of total annual discharge	% of total annual radiation
January	0.24	2.98
February	0.16	5.89
March	0.53	9.28
April	0.89	10.45
May	5.62	12.65
June	19.93	13.05
July	25.98	12.84
August	28.72	11.57
September	12.18	8.49
October	4.24	5.89
November	0.68	3.67
December	0.37	2.49

Annual records of discharge from Massa were processed and analysed for the years 2003 to 2012. Table 4.3 displays the mean annual discharge for each of these years. 2003 has the highest total discharge out of the 10 observed years; this year is recorded as a warm year due to central Europe suffering a heat wave. The all time Swiss heat record of 41.5°C was set on 11 August, 2003 (Met Office, 2015). Massa follows a typical runoff regime of a highly glacierised Alpine basin. Between the months November and March discharge levels are at the winter minima due to there being little to no meltwater and

precipitation falling primarily as snow. Maximum discharge occurs through the months June-September known as the ablation period. Table 4.2 shows the percentage of the total annual discharge for each month in 2012 from the Massa, it has a typical flow regime of an Alpine glacial basin as 86.8% of the annual total discharge was in four months; June, July, August and September with the winter months accounting for less than 10% of annual runoff. August was the highest with 28.72% of the years discharge, February the lowest with 0.16%. Mean annual water temperature for the years 2003 to 2012 are show in Table 4.4. With the exception of 2010 there is a trend of years with higher discharge possessing lower water temperatures. The year 2003 demonstrates this relationship having the highest average discharge and also the lowest average water temperatures.

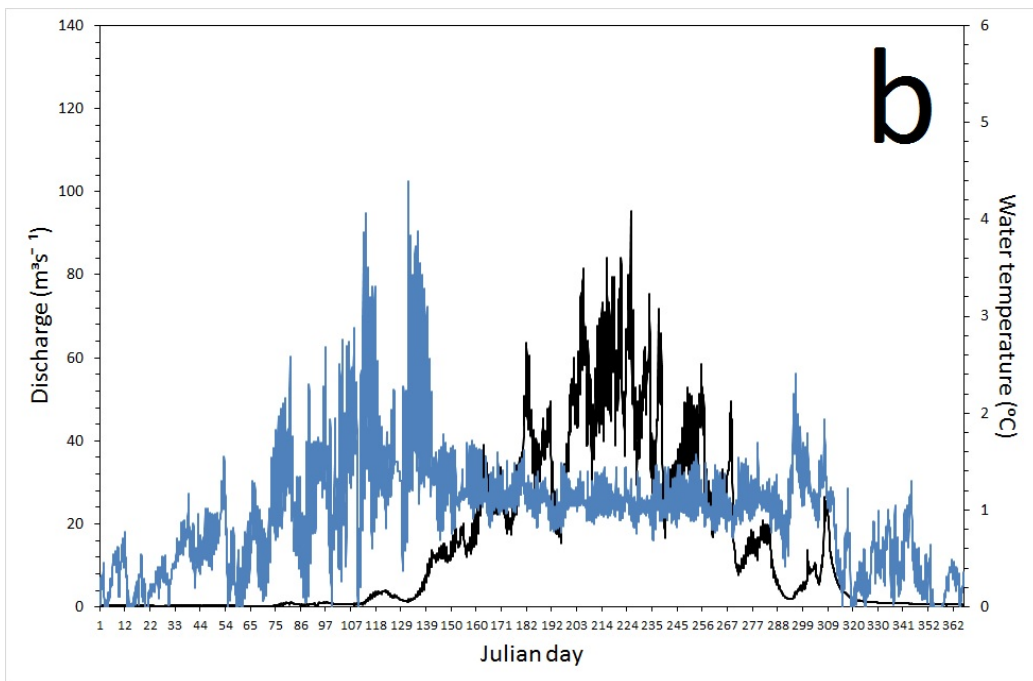
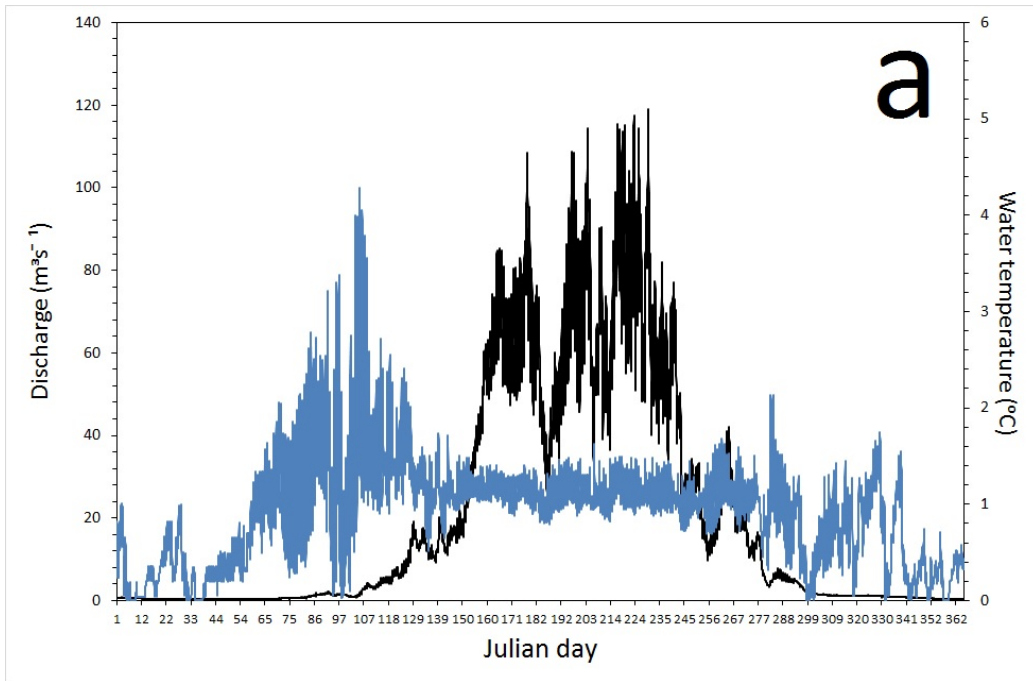
Table 4.3: Statistics of hourly discharge (m^3s^{-1}) of Massa for the period 2003-2012.

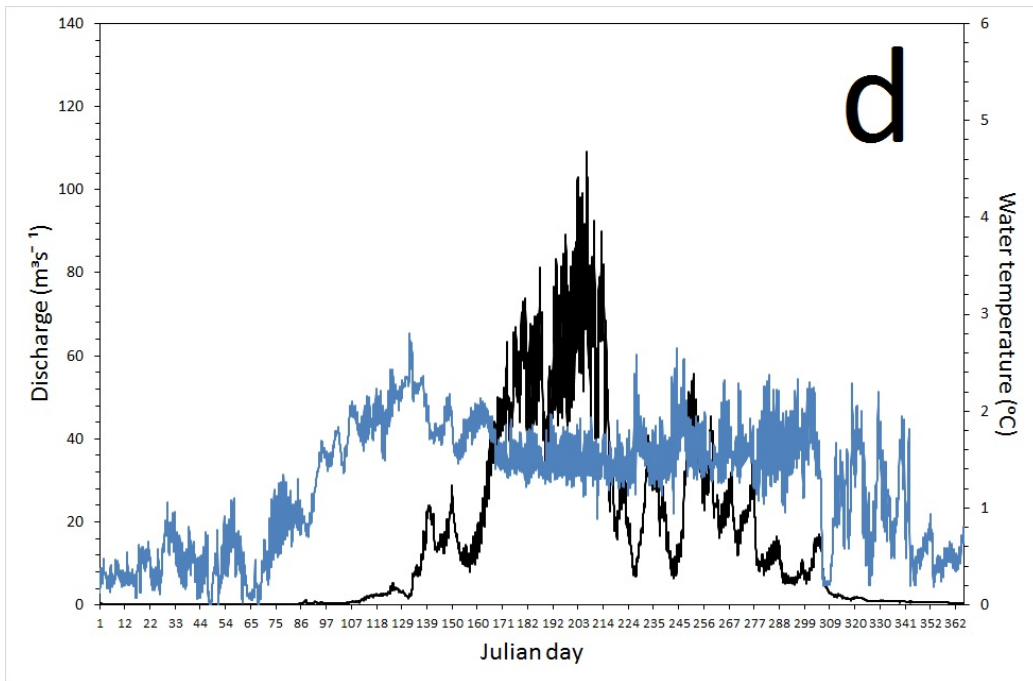
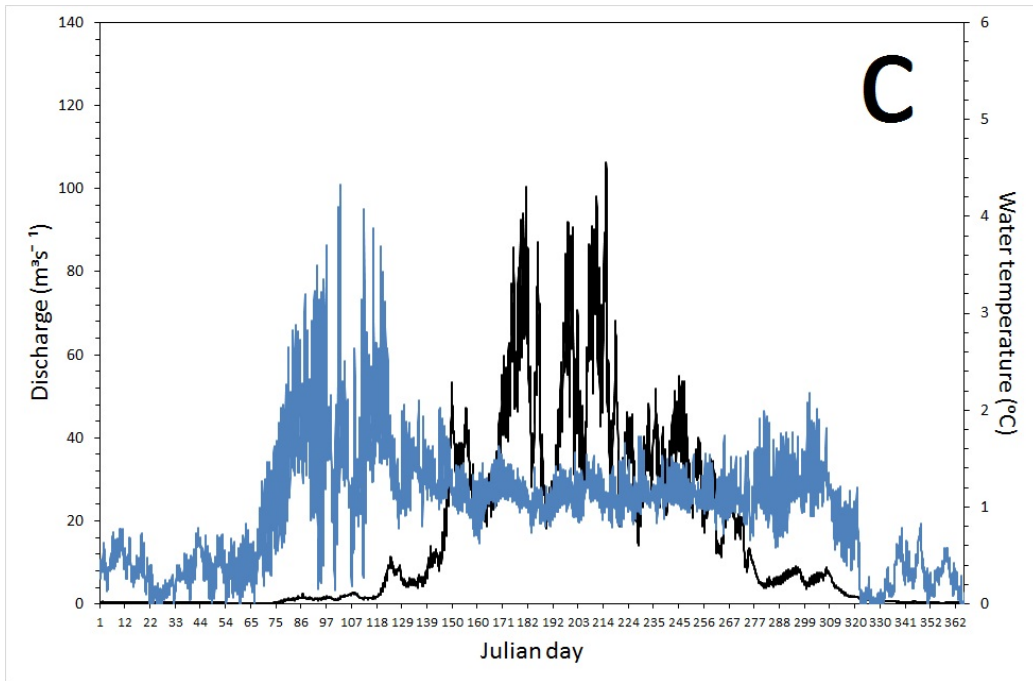
Year	Mean	Min	Max	Std. Dev.
2003	20.2	0.15	118.95	28.21
2004	14.49	0.2	95.24	19.18
2005	15.5	0.22	106.29	21.02
2006	15.07	0.06	109.07	21.26
2007	15.64	0.35	102.12	18.45
2008	15.5	0.28	108.73	21.81
2009	16.6	0.15	91.85	21.45
2010	14.2	0.19	109.12	20.55
2011	16.44	0.21	122.3	20
2012	15.96	0.14	120.82	21.28

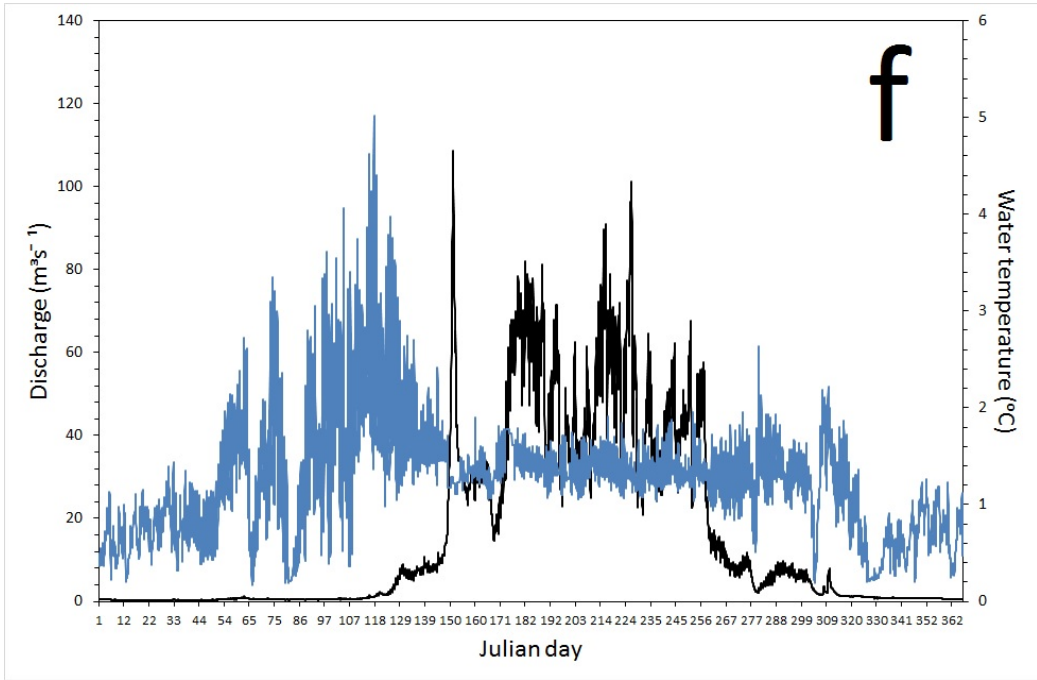
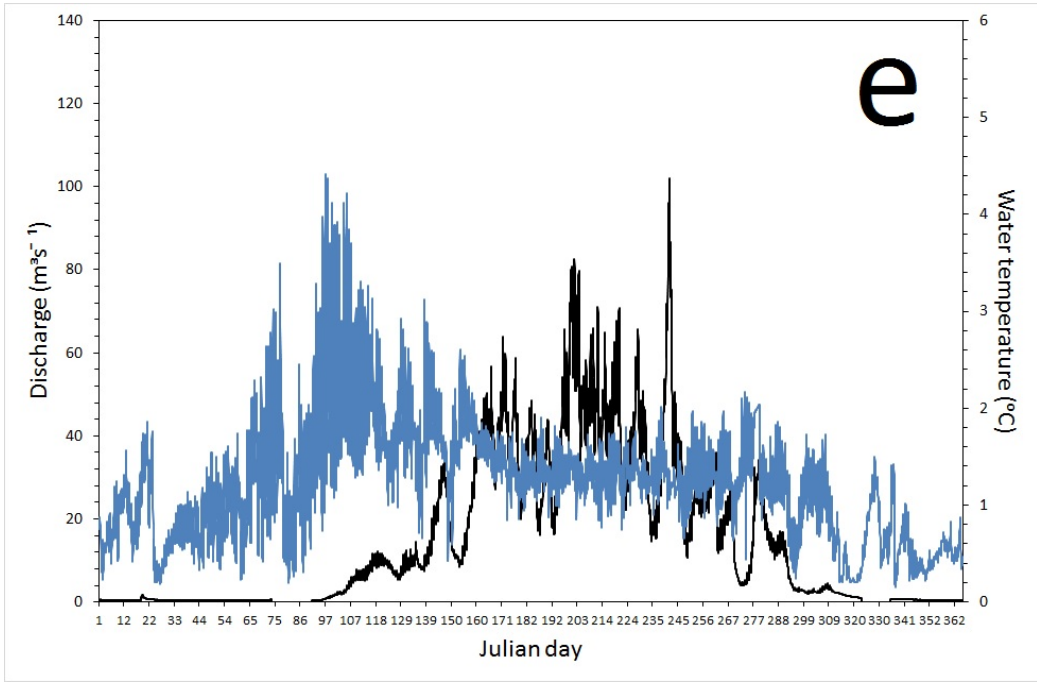
Table 4.4: Statistics of hourly water temperature ($^{\circ}\text{C}$) of Massa for the period 2003-2012. The minimum temperature has not been included due all the observed years experiencing minima of 0°C

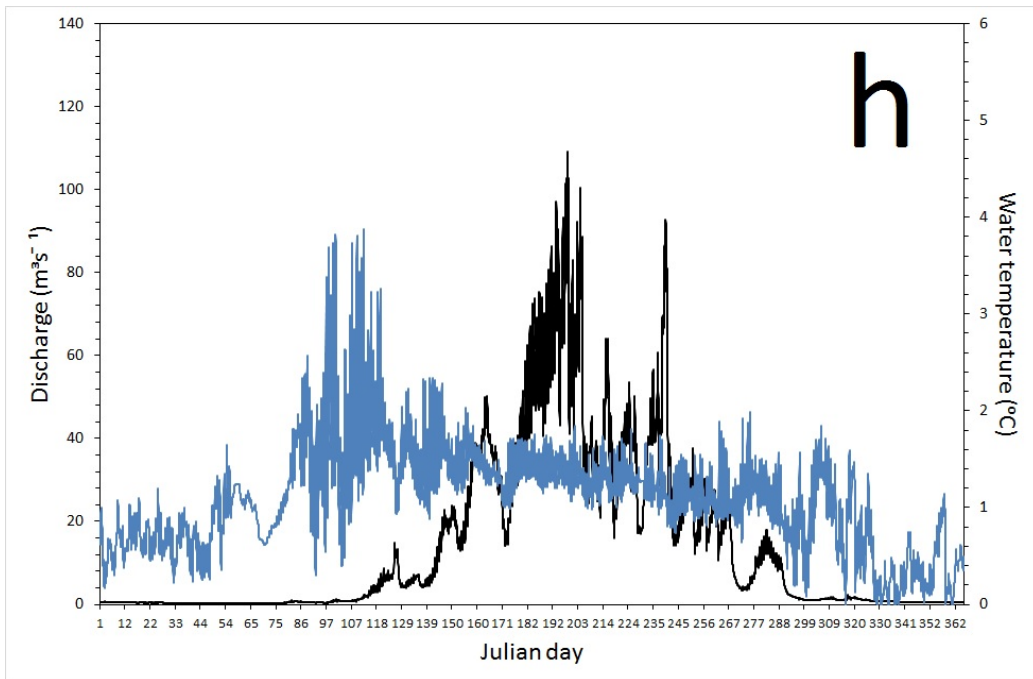
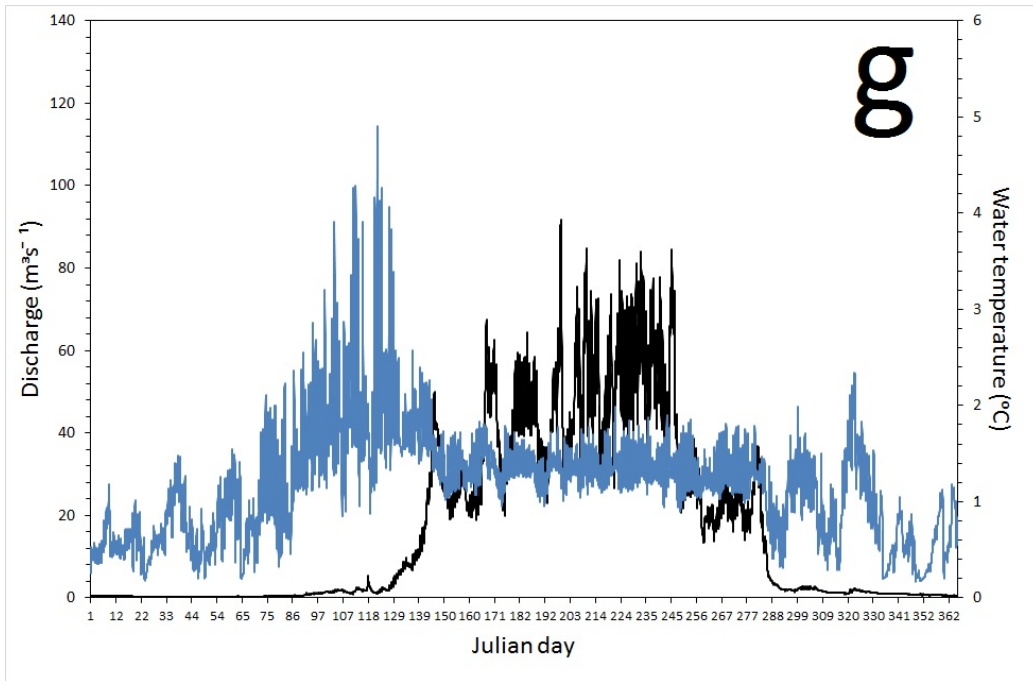
Year	Mean	Max	Std. Dev.
2003	0.89	4.28	0.51
2004	0.92	4.4	0.54
2005	0.92	4.32	0.55
2006	1.22	2.81	0.62
2007	1.18	4.41	0.57
2008	1.21	5.02	0.55
2009	1.15	4.89	0.53
2010	1.07	3.88	0.51
2011	0.93	3.82	0.46
2012	0.98	4.62	0.52

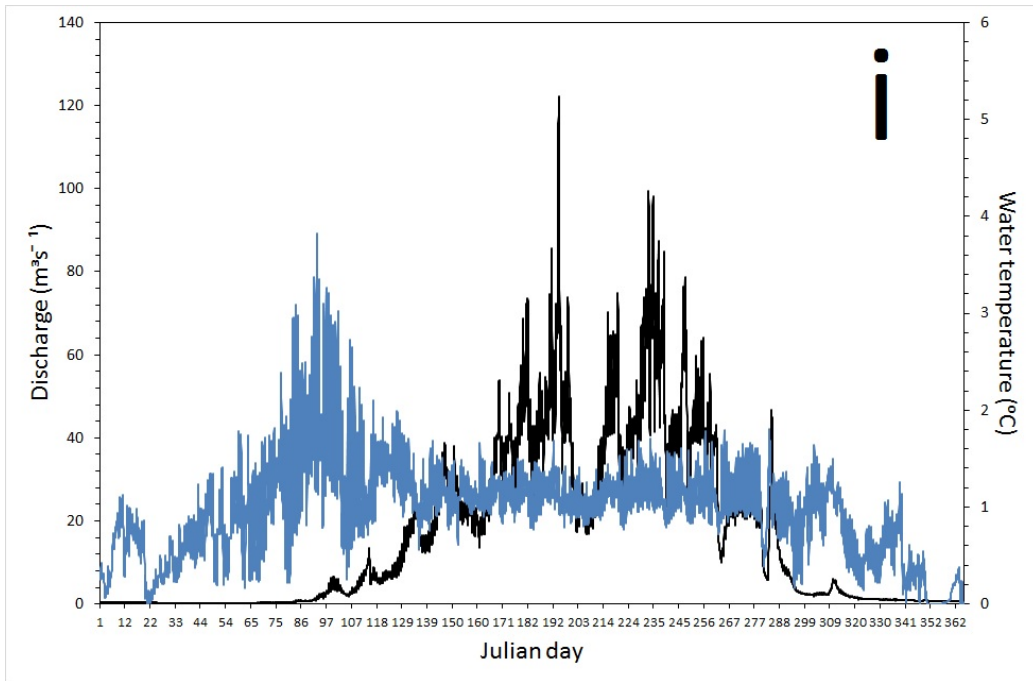
The seasonal hydrographs of water temperature (blue) and discharge (black) are shown on Figure 4.1 for the years 2003 (a) to 2012 (j). There is a similar pattern throughout the years with water temperature peaking between the Julian days 92 and 133. Figure 4.1 (j) displays the hourly data taken from the Massa, which illustrates the seasonal relationship between discharge (black) and water temperature (blue) over 2012. The hourly measurements for 2012 have been processed into seven day averages as seasonal trends for water temperature and discharge are to be analysed with radiation; which has a high diurnal range therefore this seven-day average smooths out the series for a clearer, clean observation. There is a clear apparent seasonal relationship between discharge and water temperature which can be identified throughout the years. Typically discharge is low during the winter months until the late ablation period where it rapidly increases from $7.35 \text{ m}^3\text{s}^{-1}$ in to the peak of $120 \text{ m}^3\text{s}^{-1}$ in just 45 days. Discharge continues to increase through the summer until early August when it peaks then rapidly decreases over 80 days back to low levels of winter. Discharge decreases earlier than it would be expected. Water temperature on the other hand peaks in early May when discharge is still low, but from that point there is a gradual decrease until the end of summer. There are distinctive warm water pulses in March and April which can be observed in Figure 4.1. The relationship between water temperature and discharge follow that discussed previously in which the highest periods of discharge will show a response in water temperatures decreasing.











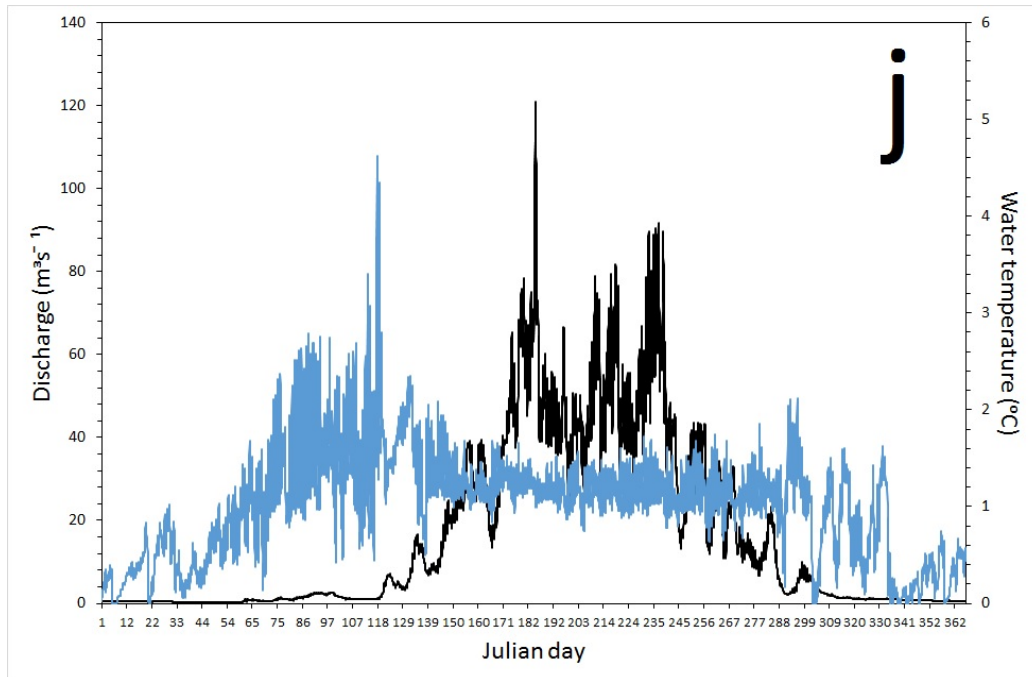


Figure 4.1: Seasonal variation of discharge (m^3s^{-1}) as the black series and water temperature ($^{\circ}\text{C}$) as the blue series of the Massa for the years 2003 (a) to 2012 (j).

Analysing the relationship between seasonal water temperature, discharge and radiation is a key objective. The year 2012 was observed in depth due to it possessing the highest total radiation over the years and it is the most recent year with complete data (see Table 4.1). Hourly data has been processed into weekly averages to give a smoother series (Figure 4.2). The point of the summer solstice has been added also to outline the longest day of the year in terms of daylight. There is a clear curve in the radiation series across the year with the peak in the week of the summer solstice, which was expected. In contrast water temperature peaks in late April, two months prior to radiation as it would be expected that a strong positive correlation would exist between these two parameters due to radiation being a major energy input in proglacial streams. This negative correlation occurs across ablation season as radiation is at its highest, and then water temperature gradually decreases after its peak. There is little response to these high radiation levels until the week of Julian day 287 where water temperature decreases at a higher rate back to the winter minima.

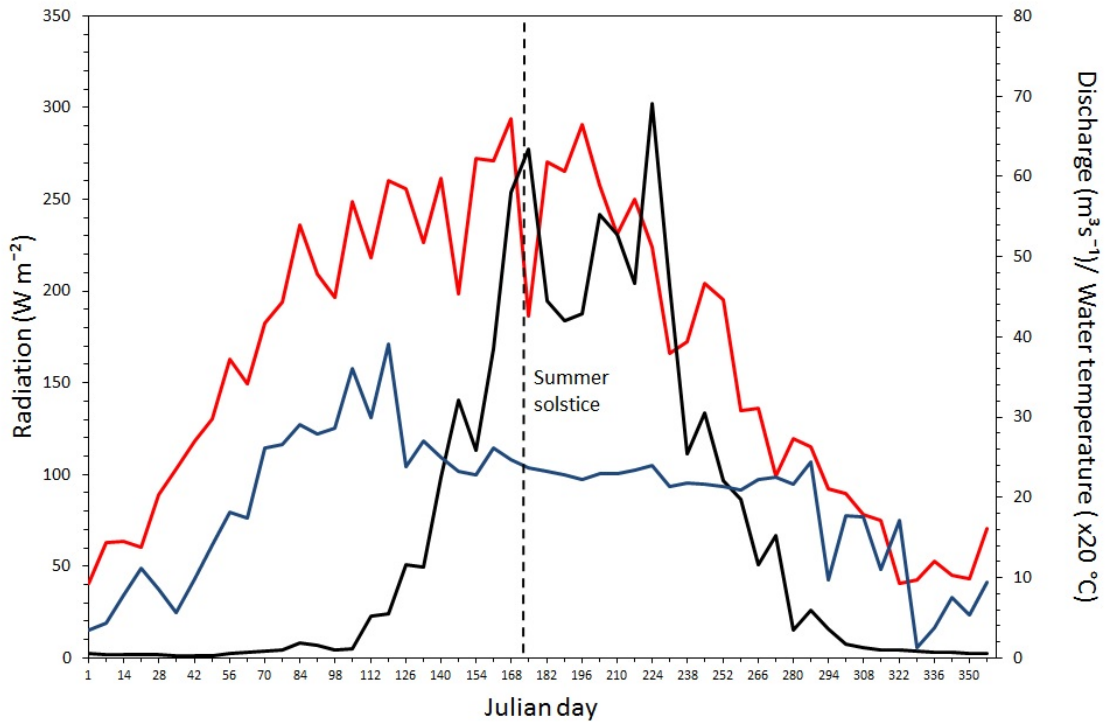


Figure 4.2: Seven day average of Massa water temperature ($\times 20 \text{ }^\circ\text{C}$) in blue, Zermatt radiation (W m^{-2}) in red and discharge ($\text{m}^3 \text{s}^{-1}$) in black of the year 2012 with the dashed line representing the summer solstice.

The monthly maximum, minimum, range and standard deviation of water temperature ($^\circ\text{C}$) for March-October 2012 for the Massa have been processed from hourly measurements (Table 4.5). The lowest maximum temperatures occur in June, July and August, which are regarded as the peak of the ablation season due to the highest temperatures. Additionally, these months host the lowest range which signify little diurnal variation in temperature. The highest maximum temperature and range occur in April, which is in the early ablation season; temperature and radiation have only begun to increase. With the range being so high this shows the month possesses a high diurnal variation in water temperature. This month shall be under close observation to analyse the diurnal variation between water temperature, radiation and discharge.

The seasonal relationship between discharge and radiation is more apparent as Figure 4.2 illustrates. This graph has been constructed with hourly measurements processed into weekly averages. As discussed radiation (red) peaks

in the week of the summer solstice which in 2012 was 20 June. In comparison, discharge has a greater rate of increase seasonally than radiation, with levels staying around the winter minima until mid-April in which the increase begins. Radiation however has a gradual rise beginning late January, with the seasonal curve clearly evident. A lag-time exists between these two parameters with the highest radiation values occurring prior to the peak discharge. Furthermore discharge is still climbing during the summer solstice and does not reach its peak until approximately 50 days later. Peak discharge for this year occurs when radiation is on the decrease, which shows that there is not an immediate response from discharge to radiation.

Table 4.5: Monthly minimum, maximum, range and standard deviation of water temperature ($^{\circ}\text{C}$) for the months March- October 2012.

Month	Max	Min	Range	Std. Dev.
March	2.79	0.14	2.65	0.47
April	4.62	0.53	4.19	0.61
May	2.35	0.5	1.84	0.37
June	1.68	0.85	0.83	0.15
July	1.57	0.75	0.82	0.14
August	1.73	0.78	0.95	0.18
September	1.74	0.64	1.11	0.2
October	2.12	0	2.12	0.42

An objective was to understand why water temperature decreases in the period when radiation is high. Water temperatures surge during the early ablation season. Figure 4.3 shows the daily average water temperature and discharge between the Julian days 91 and 152, which have been selected as this is the period in which discharge increases from its winter minima. In the period between days 91 and 116 there are large fluctuations in water temperature, but here in contrast discharge varies little and remains at a low level. Discharge begins to rise from the days 117 to 122, in response average daily water temperature decreases from 2.33°C to 1.25°C in just a period of 4 days. The trend is repeated as rising discharge shows a potential relationship with decreasing water temperatures; however temperature increases as discharge decreases from the peak on Julian day 122, average daily discharge decrease from $6.78\text{ m}^3\text{s}^{-1}$ to $3.67\text{ m}^3\text{s}^{-1}$ on day 128, in the same period water temperature increases from 1.36°C to 1.84°C . Towards the end of the observed period this trend is recognisable further, in this time frame water temperature does not surge. Furthermore stream temperature begins

to decrease as discharge continues to rise. Average daily radiation for the same period is shown in Figure 4.4, while there is much daily variation there is a clear steady increase as the added lines show. There does not appear to be a correlation with water temperature as expected.

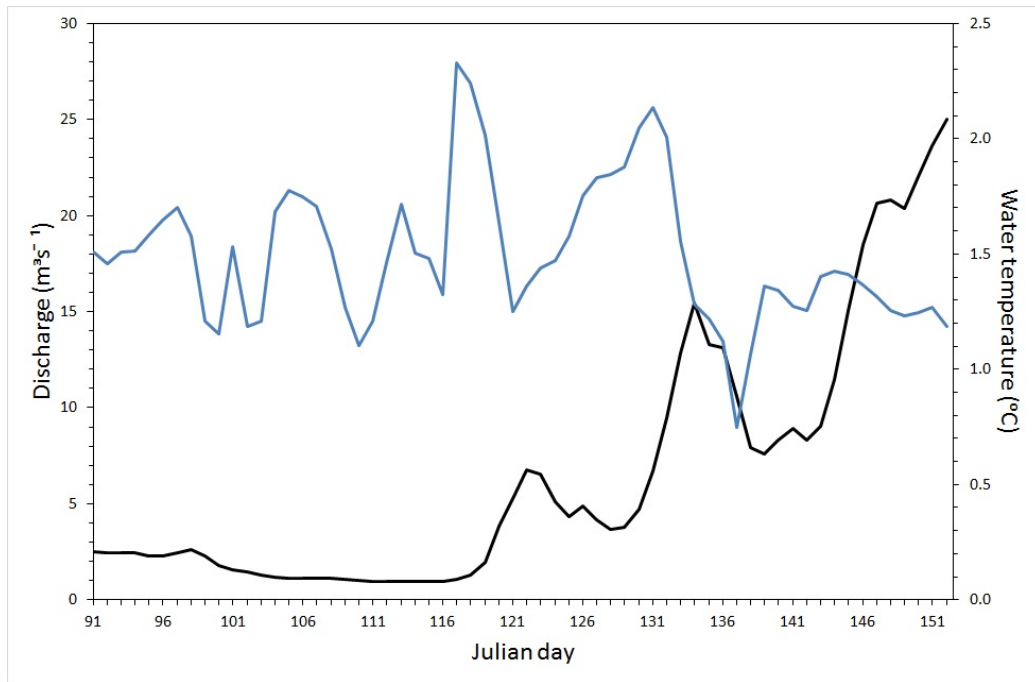


Figure 4.3: Daily average of hourly water temperature ($^{\circ}\text{C}$) in blue and discharge (m^3s^{-1}) in black for the Massa between the Julian days 91 and 152, 2012.

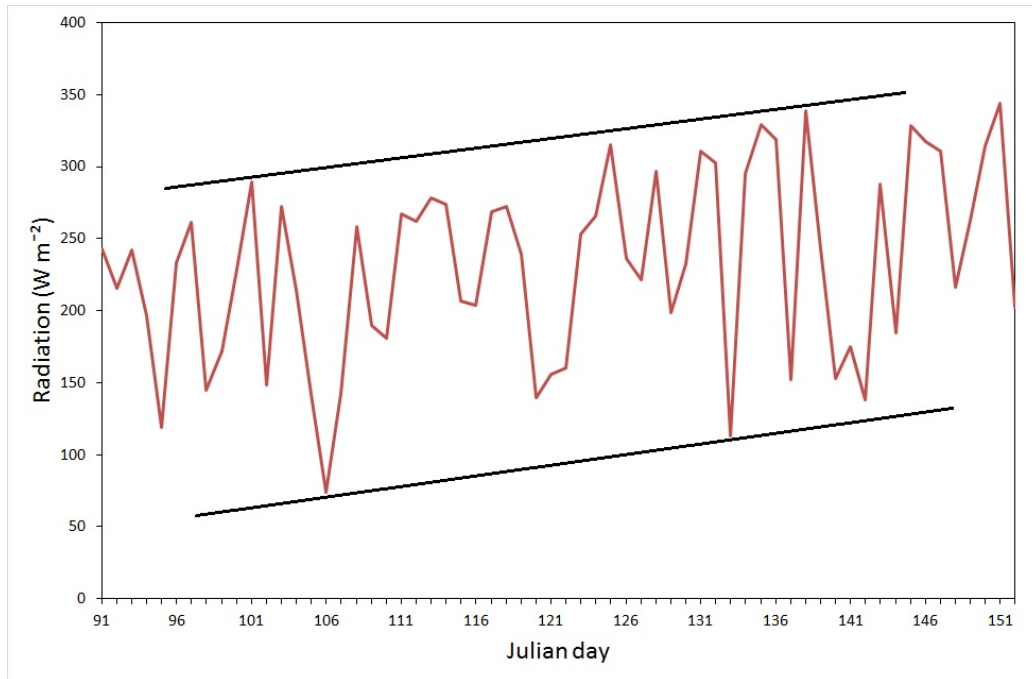


Figure 4.4: Daily average of hourly shortwave radiation (W m^{-2}) with lines added to highlight the increase of radiation over the period between the Julian days 91 and 152, 2012.

In order to determine if the trends in Figures 4.3 and 4.4 were consistent for all the years between 2003-2012 the same analysis is demonstrated in Figure 4.5 and 4.6 but this has been produced with the hourly measurements for all the years 2003-2012 averaged to form a daily basis. There is less variation in the series which produces recognisable trend between discharge and water temperature. The tipping point at which water temperature stops increasing and then begins to decrease on Julian day 116 which in a regular year is April 26th. At this tipping point the discharge level is $3.54\text{m}^3\text{s}^{-1}$. Radiation however is still steadily rising throughout this period (Figure 4.6).

The level of discharge at which stream temperatures cease to surge and decrease from the peak were determined by analysing the daily average water temperatures and outlining the point at which the decline begins. The total run off from that day and the annual total run off were calculated. Table 4.6 displays these results with the percentage of the annual total at which the daily total amounts. The highest percentages are in the years 2012 and 2006 with the lowest in 2008 and 2003. Water temperatures in 2008 decreased from the peak with only 0.02% of the annual discharge for that day while in

comparison 0.16% of the annual discharge was needed for water temperatures to respond in 2012. The percentage of the annual total discharge at which water temperatures decrease is shown in Table 4.7 for the years 2003-2012, which was calculated by the sum of the discharge from the start of the year up until the day stream temperatures decreases from the peak and cease to pulse.

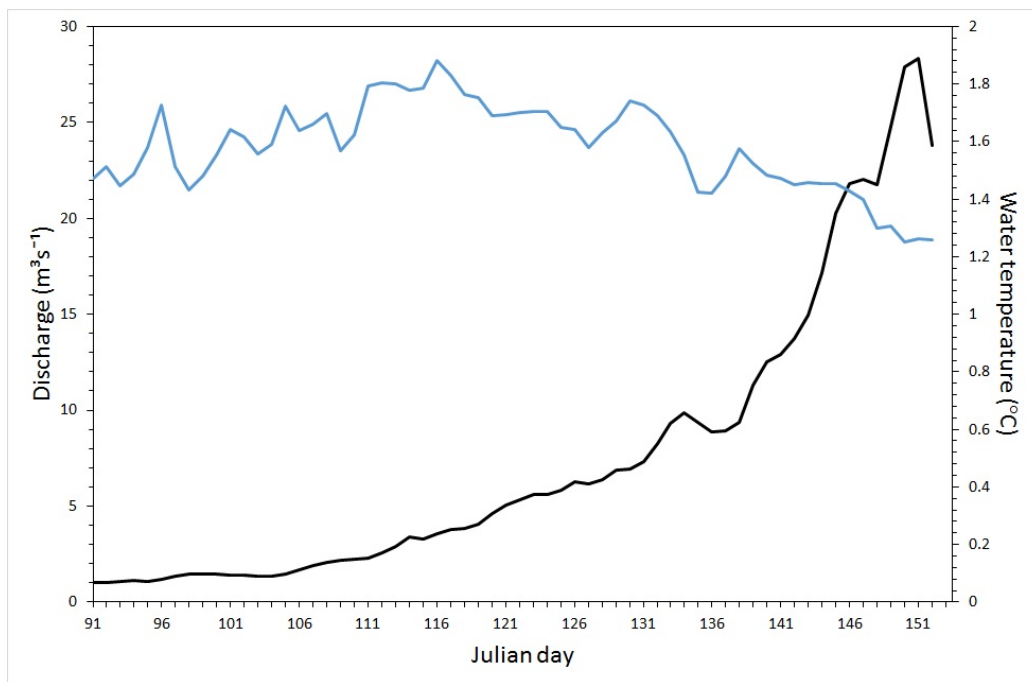


Figure 4.5: Daily average of hourly water temperature ($^{\circ}\text{C}$) in blue and discharge (m^3s^{-1}) in black between the Julian days 91 and 152, 2003-2012.

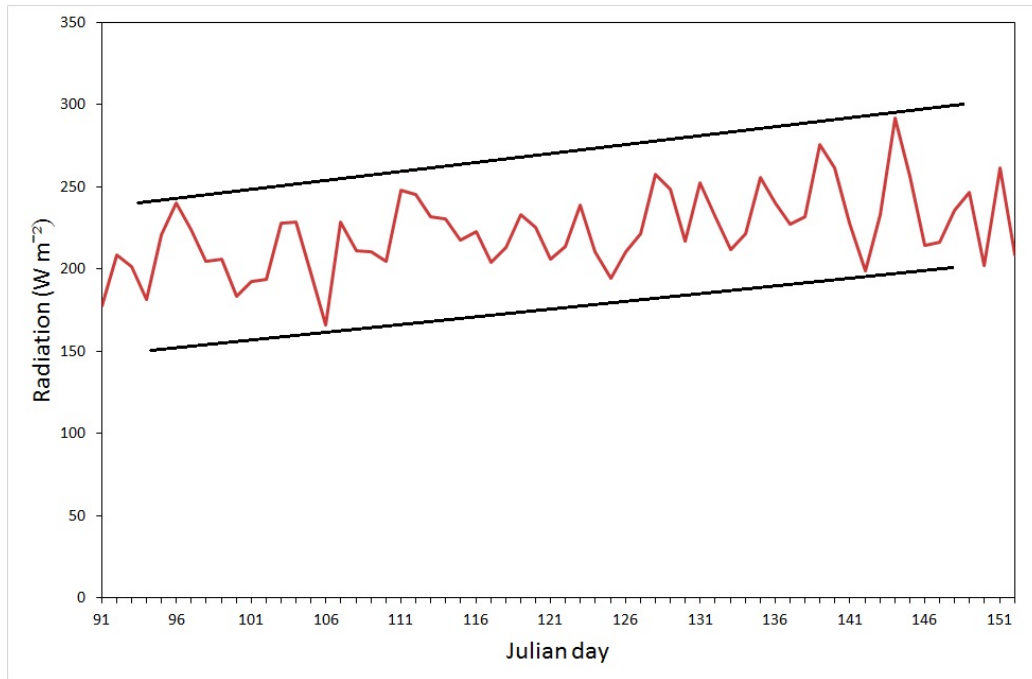


Figure 4.6: Daily average of hourly shortwave radiation (W m^{-2}) between the Julian days 91 and 152, 2003-2012.

Table 4.6: Annual total discharge (10^6 m^3) for the years 2003-2012 and the daily total of discharge from the day at which water temperature begins to decrease from the annual peak. With the percentage of the annual total added.

Year	Annual total	Daily total	% of annual total
2003	636.52	0.19	0.03
2004	458.2	0.2	0.04
2005	488.85	0.48	0.1
2006	475.07	0.59	0.12
2007	453.97	0.27	0.06
2008	490.03	0.09	0.02
2009	523.49	0.17	0.03
2010	447.79	0.5	0.11
2011	518.45	0.16	0.03
2012	504.77	0.82	0.16

Table 4.7: Total discharge (10^6m^3) from the January 1 up until the day water temperature decreases and the percentage of the annual total.

Year	Total prior to water temp decrease	% of annual total
2003	5.32	0.84
2004	9.02	1.97
2005	8.42	1.72
2006	7.98	1.68
2007	4.43	0.98
2008	4.68	0.96
2009	7.24	1.38
2010	6.42	1.43
2011	2.91	0.56
2012	13.79	2.73

The Massa experiences warm pulses in the autumn and early winter (Figure 4.1). The Julian days 285-298 were observed closely as this period possessed the peak water temperatures for the post ablation season. The hourly variations of discharge (black series) and water temperature (blue series) are shown in Figure 4.7. Discharge reduces at a high rate from $20.12\text{m}^3\text{s}^{-1}$ for day 285 to $2.51\text{m}^3\text{s}^{-1}$ on day 290, while in response water temperature fluctuates from 0.17°C to 2.12°C .

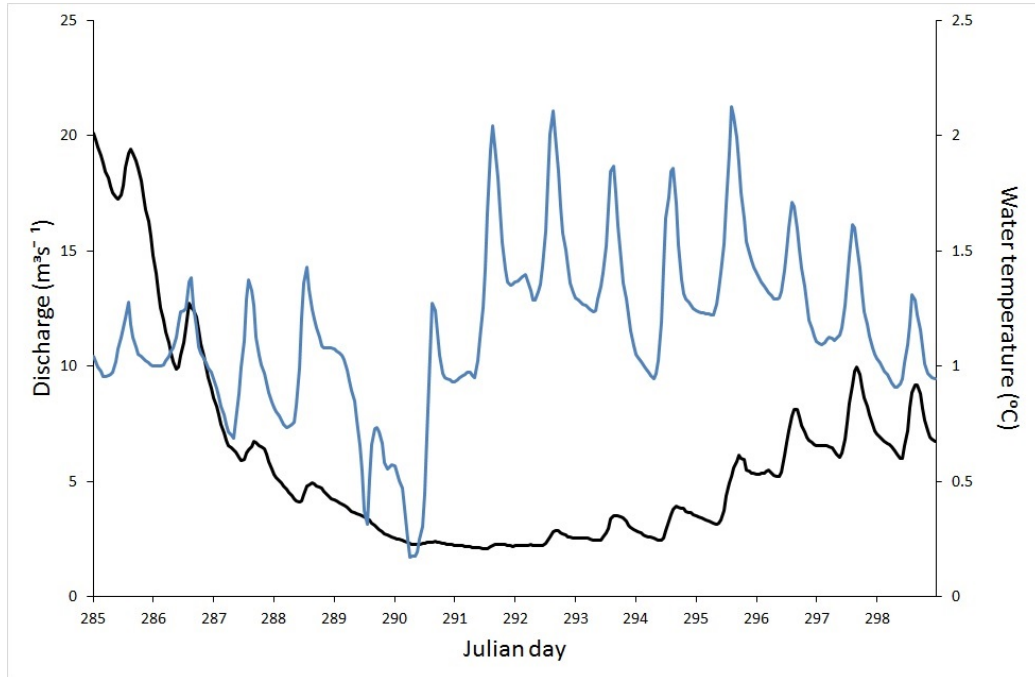


Figure 4.7: Hourly variations of discharge (m^3s^{-1}) (black) and water temperature ($^{\circ}\text{C}$) (blue) between the Julian days 285 and 298, 2012.

The hourly variation of radiation and stream temperature beginning Julian day 110 (19 April) leading up to the peak of water temperature on Julian day 117 (26 April) is shown in Figure 4.8. There is a potential pattern between both series with a lag time of a couple hours between peak radiation and peak stream temperature; however the daily maximum and minimum values express a relationship across the whole 8 days, suggesting that radiation is the primary controller of stream temperature. For comparison the day of peak radiation and the preceding week was analysed at the same resolution. Figure 4.9 displays the hourly variation between water temperature and radiation for the Julian days 150-158. Radiation levels are higher, however water temperature deviates little with a standard deviation of 0.16 compared to the days 110-117 that has a standard deviation of 0.79. The discharge for these periods are shown in Figures 4.10 and 4.11, which illustrate that levels are considerably higher for the period 150-158 in comparison to 110-117 where levels demonstrate the winter minima. The data series for Figures 4.8 and 4.9 were plotted with both axis values the same in order to demonstrate the decrease of water temperatures during peak radiation. These results determine radiation to be a major control of stream temperature in the ablation season; contrastingly in the summer it has a reduced influence on stream

temperature.

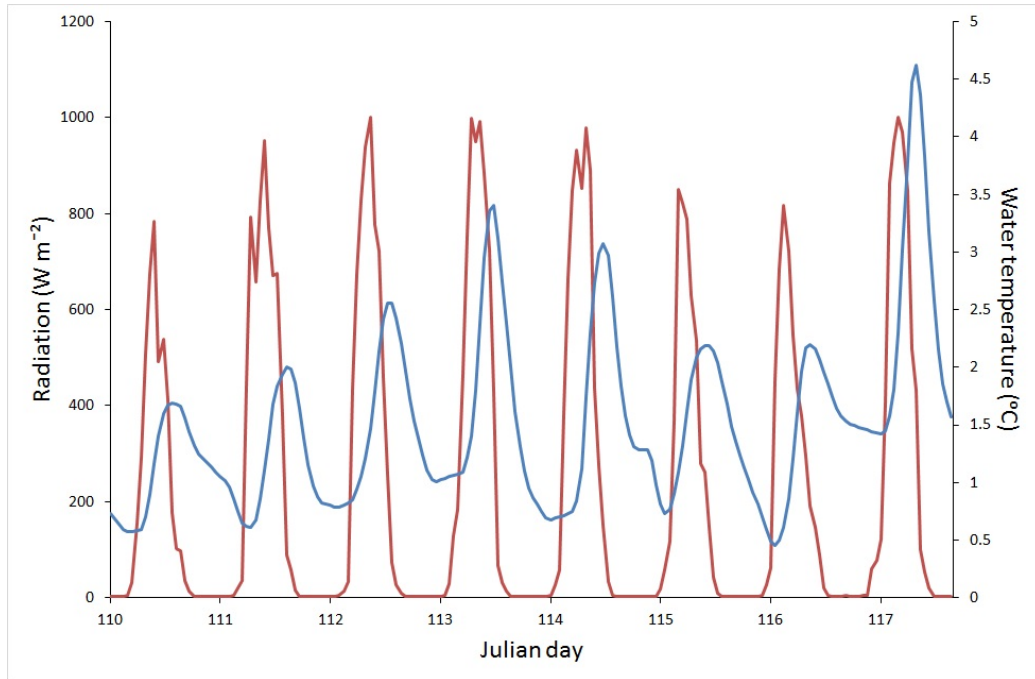


Figure 4.8: Hourly variations of radiation (W m^{-2}) (red) and water temperature ($^{\circ}\text{C}$) (blue) between the Julian days 110 and 117, 2012.

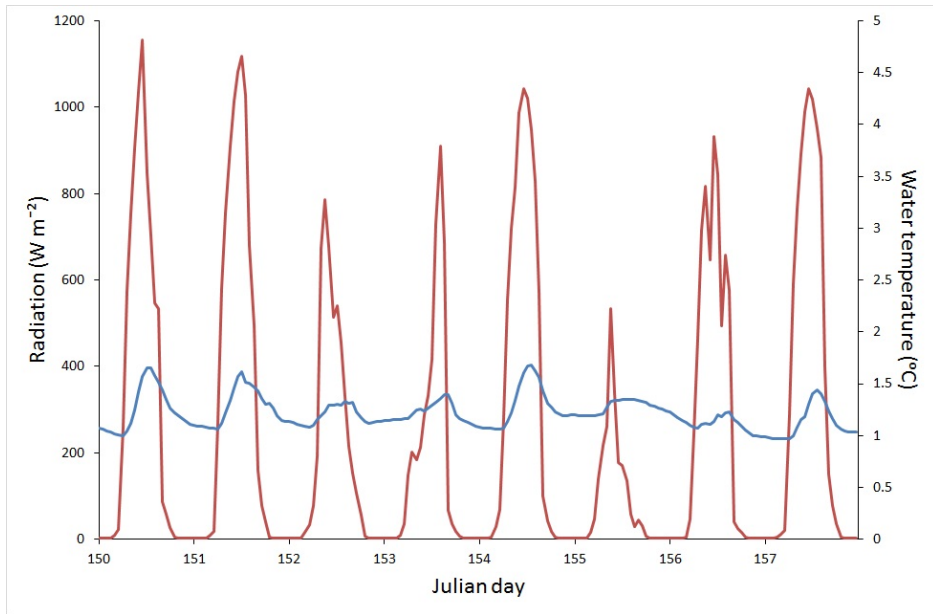


Figure 4.9: Hourly variations of radiation (W m^{-2}) (red) and water temperature ($^{\circ}\text{C}$) (blue) between the Julian days 150 and 158, 2012.

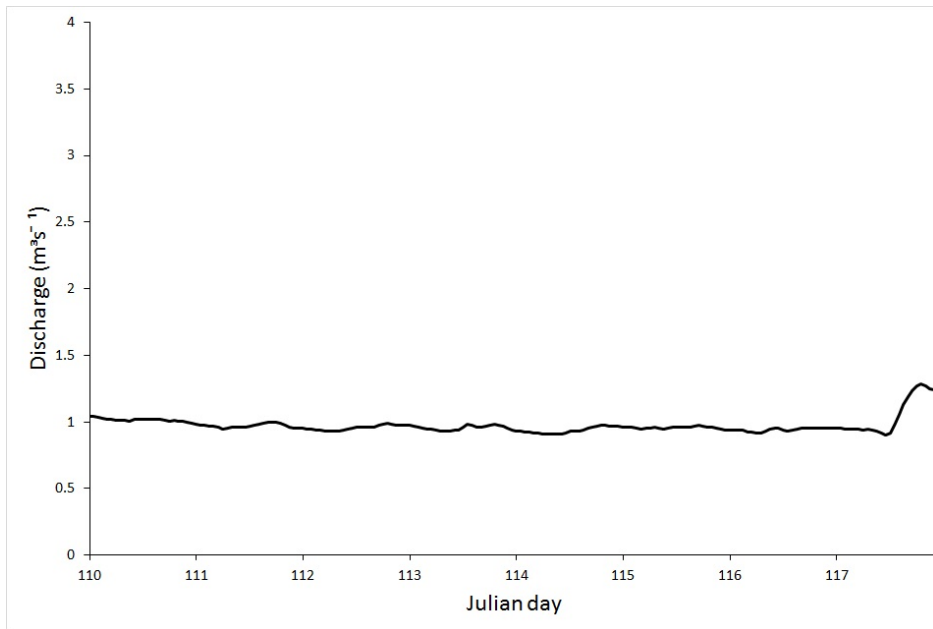


Figure 4.10: Hourly variations of discharge (m^3s^{-1}) between the Julian days 110 and 117, 2012.

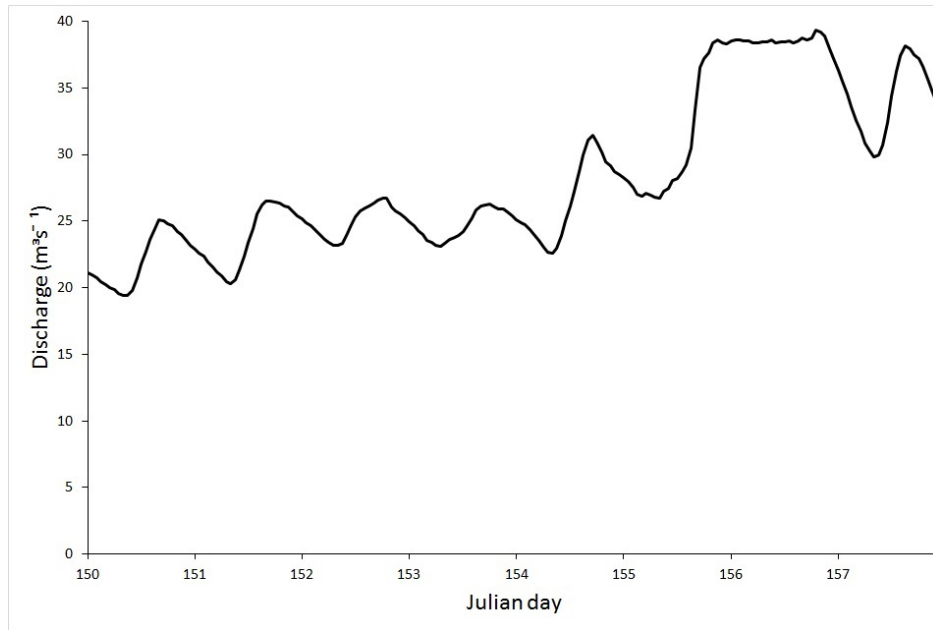


Figure 4.11: Hourly variations of discharge (m^3s^{-1}) between the Julian days 150 and 158, 2012.

4.2 Diurnal variation

The early ablation season is the principle focus of the research as stream temperatures surge and peak whilst radiation levels are still low. The hourly measurements of water temperature and discharge were compared to assess the transforming relationship over four weeks in 2012. Starting 14 May and ending 4 June, four single days exactly a week apart from each other were assessed. This period was chosen because average stream temperature begins to decrease. Figure 4.12 display hysteresis plots for each of these days. The first of the series shows a loop with a tall flat shape, there is little diurnal variation in discharge with the range only $2.76\text{m}^3\text{s}^{-1}$. In contrast there is a high variation in temperature ranging between $0.82\text{-}1.89\text{ }^\circ\text{C}$, over $1\text{ }^\circ\text{C}$ of temperature change in a single day. Out of the four days assessed 14 May possessed the highest temperature. The 21 May shows a similar shape to that of the week before however with a much decreased range in water temperature with it only ranging between $1.12\text{-}1.52\text{ }^\circ\text{C}$. Also discharge is much lower, with the peak of the day only $8.92\text{m}^3\text{s}^{-1}$, with a range of only $1.13\text{m}^3\text{s}^{-1}$. Graph (C), the third week of the observed period, still follows the trend of a thin, stretched loop. However, there is a clear increase of discharge with associated

diurnal variation. The mean discharge for this day is $20.39\text{m}^3\text{s}^{-1}$ with a range of $4.58\text{m}^3\text{s}^{-1}$. These values are much higher than the previous two weeks. The temperature of this day ranges from $1.06\text{ }^\circ\text{C}$ to $1.57\text{ }^\circ\text{C}$, which is lower than the previous week and the range and maximum temperature are higher. However, on mean the hourly water temperature for the day is slightly cooler at $1.23\text{ }^\circ\text{C}$. Figure 4.12 (D) illustrates a sudden increase of discharge for that day compared to the week before. The mean flow for the day is $38.51\text{m}^3\text{s}^{-1}$, almost a 100% increase of the discharge from Figure 4.14 (C). The range is narrower at $2.13\text{m}^3\text{s}^{-1}$, the height of the loop illustrates this. Contrastingly water temperature is far lower. The minimum has dropped just below $1\text{ }^\circ\text{C}$ and the maximum has decreased to $1.23\text{ }^\circ\text{C}$. The range is considerably low with the temperature only differing $0.24\text{ }^\circ\text{C}$ throughout the day.

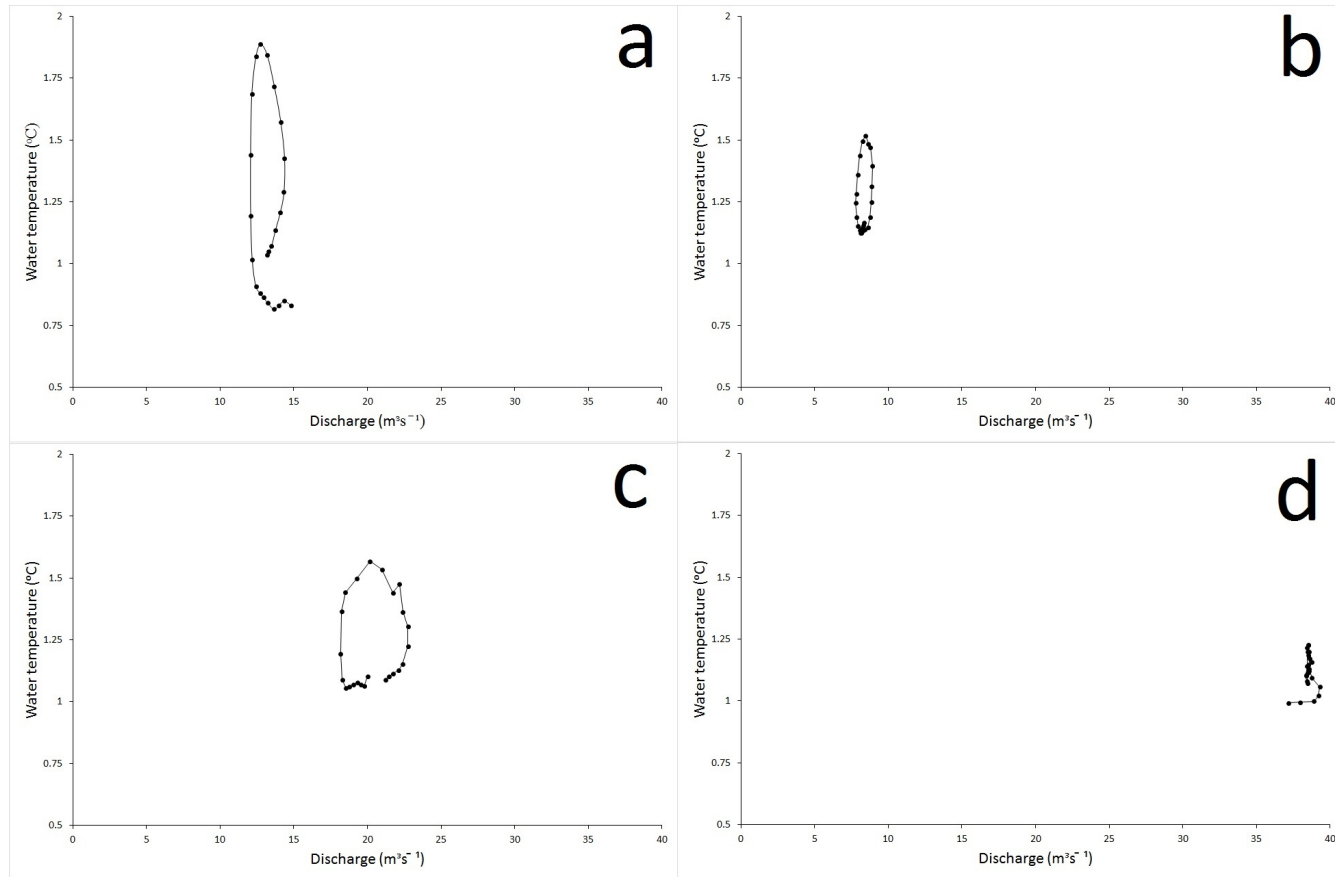


Figure 4.12: Hysteresis plots of the hourly diurnal variation of water temperature ($^{\circ}\text{C}$) and discharge (m^3s^{-1}). Each graph at weekly intervals between the dates 14 May and 4 June 2012. 14 May (A), 21 May (B), 28 May (C) and 4 June (D).

The diurnal variation of solar radiation, discharge and water temperature is shown in Figure 4.13. These particular measurements are for 26 April 2012 as this is the day of peak water temperature, and the trends reflect those of a typical glacier fed Alpine stream. There is an expected lag time between peak radiation at 11:00 and peak discharge at 19:00 due to the length of time the melt water takes to be released from the glacier's terminus. Water temperature has a lag time of 4 hours following peak radiation and decreases as discharge levels reaches $1.13\text{m}^3\text{s}^{-1}$.

Hysteresis plots were also generated for radiation and water temperature to demonstrate the diurnal relationship between the two. Figure 4.14 show the diurnal variation of water temperature and radiation for the Julian days 117(a) and 185 (b). These days were selected to signify the contrast between a day in the early ablation period when water temperature surges and a day during the peak ablation season when discharge and radiation are at their highest. There is a clear difference between the water temperature with graph (a) resembling a high diurnal variation with a minimum temperature of $1.42\text{ }^\circ\text{C}$ and a maximum of $4.62\text{ }^\circ\text{C}$, while in contrast (b) had a lower minimum and maximum temperature of $1\text{ }^\circ\text{C}$ and $1.35\text{ }^\circ\text{C}$. The diurnal pattern was similar however with temperatures peaking around 14:00-15:00. The diurnal variation of radiation for both days was expected with peak levels around midday and at a similar level with (b) possessing a slightly higher peak of 1048 W m^{-2} compared to 1000 W m^{-2} , however (a) possessed a total of 1022 W m^{-2} which is greater than (b).

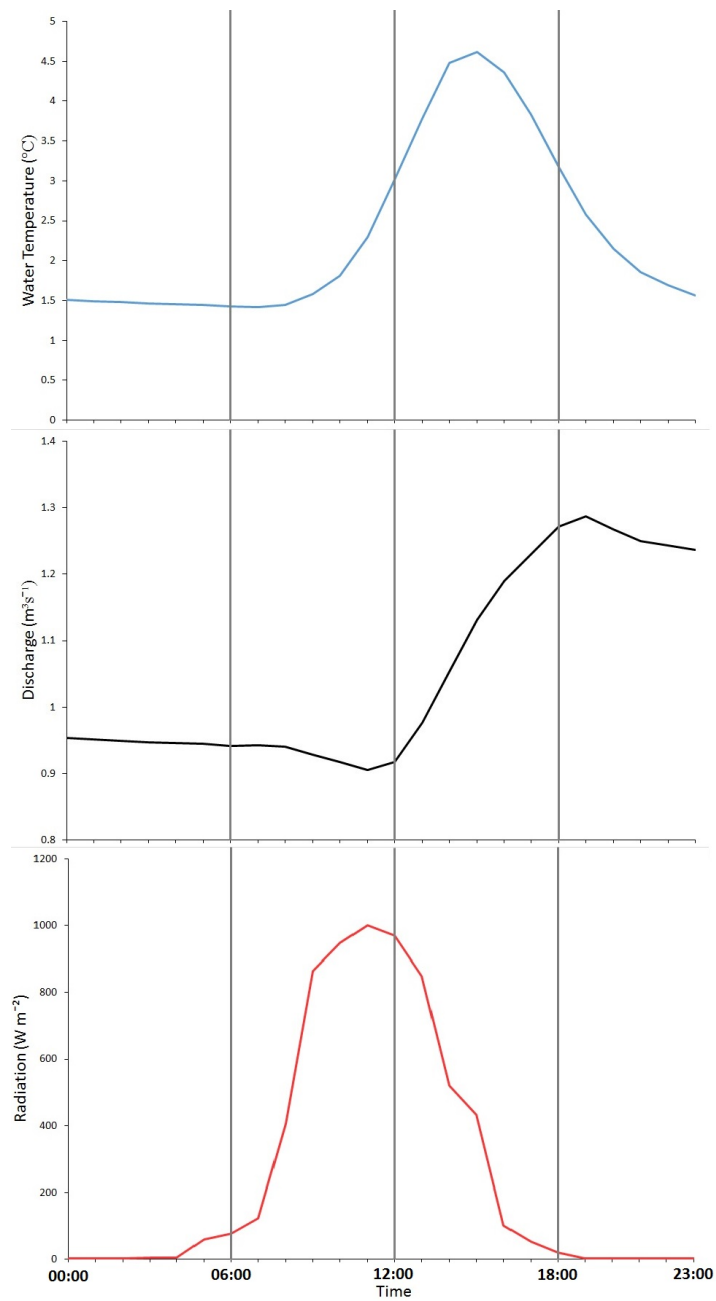


Figure 4.13: Diurnal variation of water temperature ($^{\circ}\text{C}$), discharge (m^3s^{-1}) and shortwave radiation (W m^{-2}), for 26 April 2012.

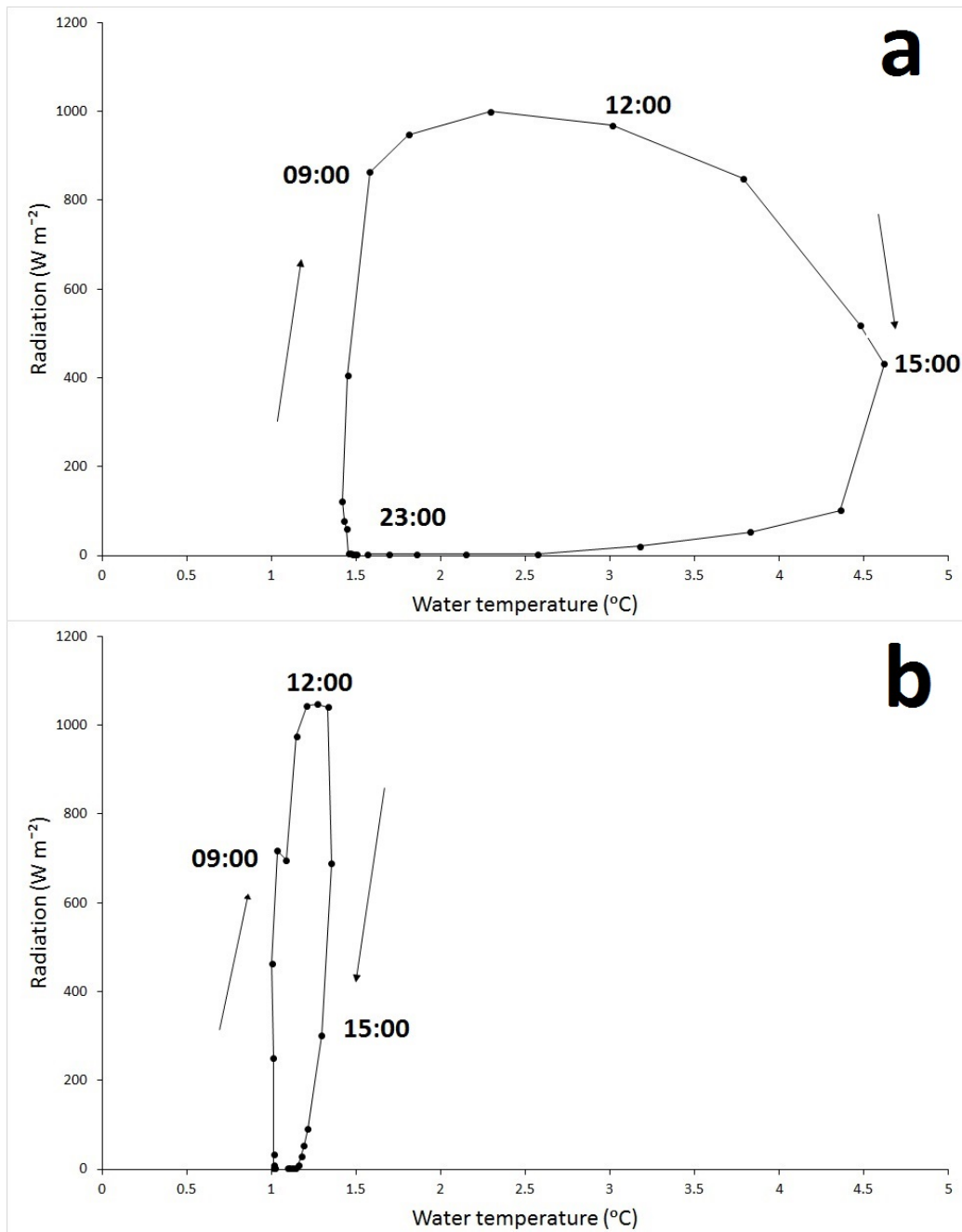


Figure 4.14: Hysteresis plots of shortwave radiation (W m^2) and water temperature ($^{\circ}\text{C}$) for the dates 26/04/2012 (a) and 03/07/2012 (b). Key times and arrows added to indicate temporal variation.

In conclusion for this period under close observation, the overall diurnal

pattern indicates that as discharge increases water temperature decreases. Figure 4.12 (D) displays this well, illustrating that the day with the highest recorded discharge also has the lowest recorded temperatures. Additionally, there is a positive relationship between the diurnal variation of these two parameters as when there is a high range between minimum and maximum daily discharge the same can be said with water temperature vice-versa. To display the evolution of the hysteresis loops throughout the period the same axis was used for all four graphs, however due to the high range between all four the true shapes of the loops are misrepresented. Figure 4.15 displays the measurements for 14 May however at an axis which complements the range of data. A different axis was used for the comparison with the other dates because it illustrates the different levels of water temperature and discharge. Arrows have been added to aid the direction of the measurements through the day, although it is not a perfect loop it still shows well the diurnal variation of water temperature and discharge and the strong relationship they possess with one another.

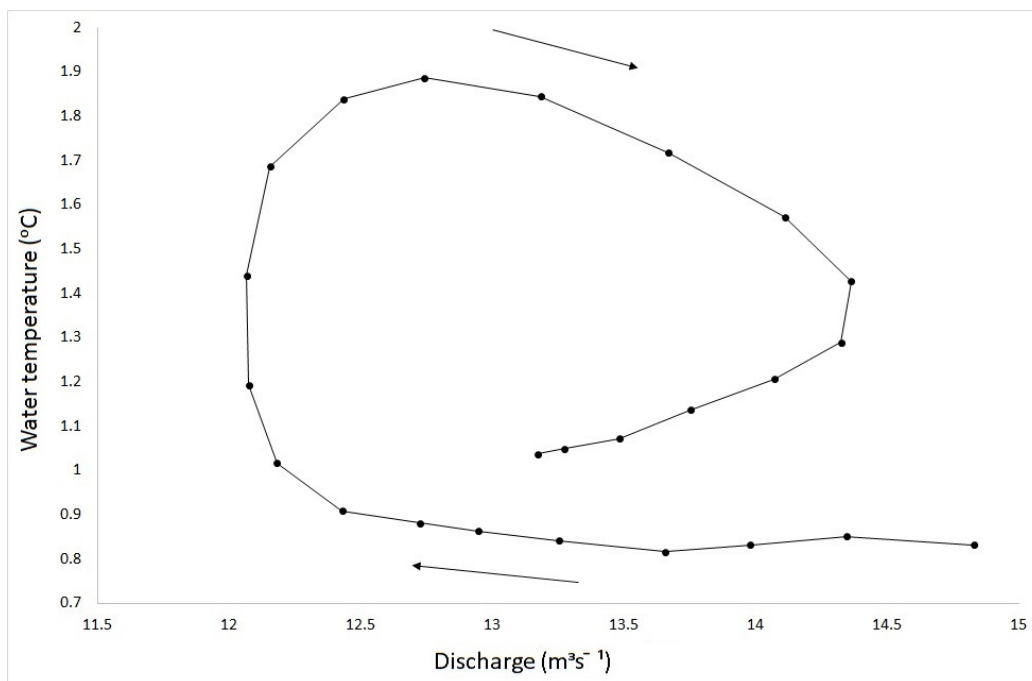


Figure 4.15: Hysteresis plot of diurnal variation of water temperature ($^{\circ}\text{C}$) and discharge (m^3s^{-1}) for 14 May 2012 of the Massa, with the direction of the series represented by the arrows.

5

Discussion

The results demonstrate a high temporal variation in water temperature and discharge of the Massa, which is similar to other studies focussing on glacier-fed streams (Brown *et al.*, 2006; Collins, 2009). Radiation followed the expected seasonal curve with the maximum levels near the summer solstice (20 June). The basin has responded to climatic warming, with Aletschgletscher retreating significantly in the last 140 years. The results suggest that stream temperature is also sensitive in this environment and very much a function of incoming solar radiation and the level of flow (Constantz, 1998; Magnusson *et al.*, 2012).

5.1 Seasonal trends

Solar radiation has been highlighted as the primary energy input of proglacial streams (Chikita *et al.*, 2010; Webb *et al.*, 2008). Analysis of the seasonal variation of thermal regimes of the Massa (Figure 4.2) conclude that water temperature increases with the radiation curve from January until the end of April. In Figure 4.2 between the months of March and May 2012 weekly average shortwave radiation and water temperature correlate strongly with $r^2=0.82$ ($p=0.002$). This is consistent with the hypothesis that solar radiation is a primary parameter determining the thermal regime of Alpine water (Brown *et al.*, 2006; Sommaruga, 2001). However water temperature peaks 33 days prior to radiation at this point the stream is cooler and no longer experiencing warm or cool pulses, which signifies the determining influence runoff has on water temperature.

As the ablation season extends into late May and June (2003-2012) runoff has an enhanced influence on the summer thermal regime of the Massa. Water temperature starts decreasing from its peak when daily average discharge increases to approximately $3.5\text{m}^3\text{s}^{-1}$ (Figure 4.5), from this point the stream is cooler and no longer experiencing warm pulses instead possessing the minimum hourly temperature range illustrated in Figure 4.1 (j). Table 4.5 expresses this well showing the range of water temperature at the lowest in summer months June-September in the year 2012. $3.5\text{m}^3\text{s}^{-1}$ demonstrates the approximate daily average level of flow at which the Massa reaches a heat capacity that stream temperature is not determined by direct solar radiation but by discharge. This supports the interpretation that water temperature is primarily a function of discharge as radiation levels are at it's yearly peak in this period.

Water temperatures not only surge in early spring but also at the climax of the ablation season when discharge levels decrease. Figure 4.7 compares the hourly trends between water temperature (blue) and discharge (black). Water temperatures surge when discharge reaches approximately $2.3\text{m}^3\text{s}^{-1}$. Day 295-298 signify the adverse relationship between the two parameters as water temperature decreases as discharge rises, reflecting the trends in Figure 4.5. Stream temperature is higher in early spring and Autumn due to groundwater having a significant contributor to runoff, this source of water is warmer than meltwater therefore prior to the ablation period water temperatures will surge when meltwater is minimal (Milner *et al.*, 2009).

Figure 5.1 provides a schematic plot of the monthly trends of water temperature, discharge and radiation with the point of the summer solstice added from the years analysed. The lag between peak radiation and discharge is because the earth absorbs radiation before releasing it into the atmosphere therefore not immediately increasing air temperatures which drive melt. The highest recorded water temperatures are when discharge is lowest due to the stream heat capacity decreasing, as reflected in Figure 5.2. During the highest discharge levels, water temperature is also generally low as the scatter shows. There is no real correlation between these two parameters with $r^2=0.08$ ($p=2.18 \cdot 10^{-162}$).

The hysteresis plots in Figure 4.15 demonstrate how radiation in summer (3 July) has a reduced diurnal influence on stream temperature compared to a day in spring (26 April). Although both show similar trends there is a large difference in the range, minimum and maximum of the days even though (b) has a higher total level of radiation. The significant differing factor between the two days is the total discharge with (a) experiencing $25.32\text{m}^3\text{s}^{-1}$ and

(b) $1821.59\text{m}^3\text{s}^{-1}$, which supports the interpretation that an increased runoff generated from snow and ice melt significantly controls the water temperature even though radiation is at its highest due to a shift in the main contributing water source, an increased heat capacity and reduced residence time.

Tables 4.6 and 4.7 express how an insignificant proportion of the annual runoff can have an effect on stream temperatures. Water temperature diversely react to a small proportion of the total annual runoff with the stream temperatures reducing from their peaks on days with a total runoff between 0.02% and 0.16% of the annual total. The amount of runoff between the start of the calendar year and the day in which water temperatures decrease from their spring peak is low with only 0.56%-2.73% of the total annual discharge occurring (Table 4.7), which signifies how the thermal regimes of glacier-fed Alpine streams are very much controlled by runoff.

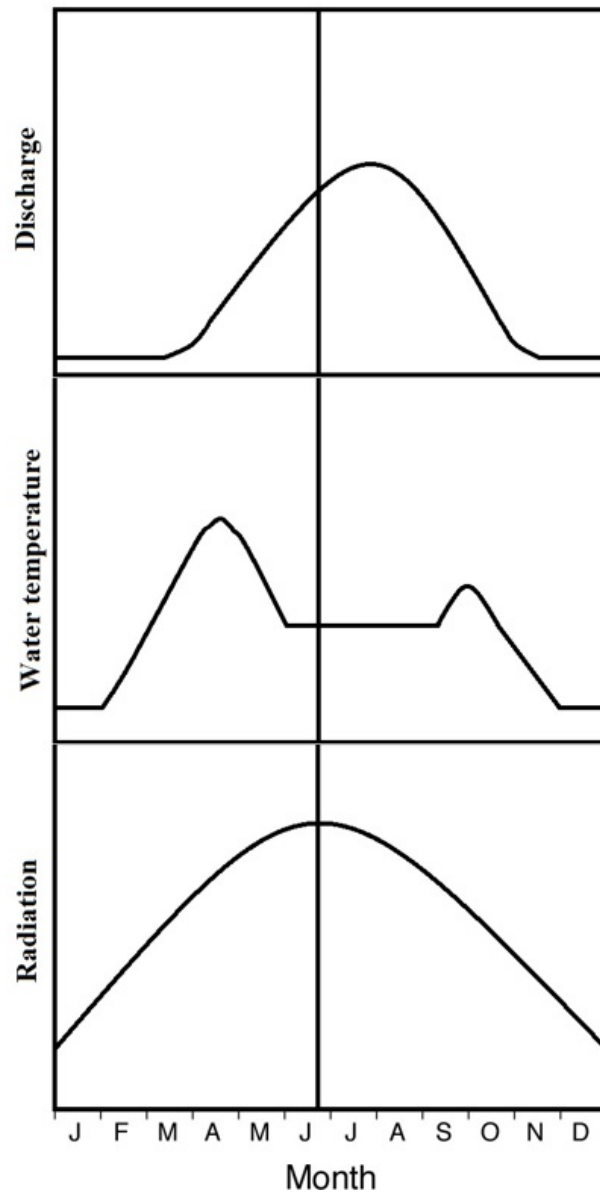


Figure 5.1: Schematic representation of monthly variations of water temperature, discharge and radiation. With the point of the summer solstice added.

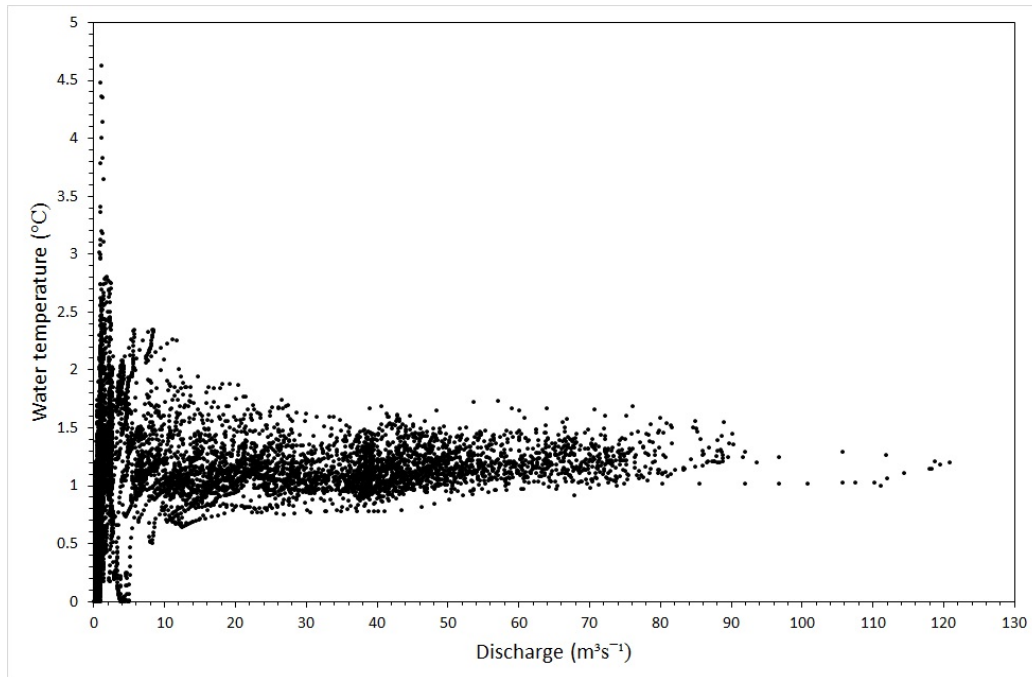


Figure 5.2: Plot of the hourly discharge (m^3s^{-1}) and water temperature ($^{\circ}\text{C}$) for Massa 2012.

5.2 Diurnal trends

The results have suggested that the diurnal variability of discharge determines the thermal regime of glacier-fed streams on a diurnal basis. As discharge increases through the early ablation season the diurnal range of water temperature decreases (Figure 4.12). Not only does the variation decrease but the mean temperature also is reduced. Hysteresis plots are appropriate for analysing temporal variation of hydrological data on diurnal scale as it highlights patterns cyclically. The tall, narrow cycles (Figure 4.12 (a)) situated close to the Y axis signify days in which discharge has a low diurnal variation and reduced maximum. Figure 4.14 demonstrates the transforming patterns of the diurnal variation of discharge and stream temperature significantly, the loops laterally move across the plot and reduce in size as the weeks progress, this signifies how higher discharge reduces the variability of stream temperature. This is due to a higher volume of water in which increases velocity of the stream therefore reducing the transit time through the proglacial environment.

Lag times exist between the peaks of each variable on a diurnal basis (Figure 4.8). Water temperature peaks in the early afternoon and discharge in the evening, this suggests that water temperature responds rapidly to atmospheric variation. Discharge lags radiation due to the delayed drainage of meltwater exiting Aletschgletscher; these diurnal patterns are consistent with previous studies of glacier-fed streams (Constantz, 1998; Constantz *et al.*, 1994). Stream temperature does not vary significantly at night, suggesting that stream bed friction is maintaining the constant temperature.

5.3 Stream morphology and topography

River morphology and basin topography have to be taken into consideration as these have proven to be complex in proglacial fields and determine the variability of runoff and thermal regimes (Magnusson *et al.*, 2012). The Massa is a typical proglacial Alpine stream with expected topography and river morphology of a highly glacierised basin. This includes it possessing a boulder dominated channel, areas of steep sided V shaped channels, high gradients and high levels of suspended sediment that lead to the development of braided channels (Maizels, 1979). Distance between the glacier terminus and gauging station is increasing yearly, as these glaciers retreat the influences of meteorological will be greater (Chikita *et al.*, 2010). Areas of the Massa flow through a steep sided valley and gorge prior to the downstream gauging station (Figure 5.3), and so the water temperature will have limited energy input from solar radiation due to shading and narrow deep channels. Figure 4.10 illustrates the significant effect the topographical shading can have on the thermal dynamics of Alpine streams due to radiation being a primary energy input. Stream bed friction is limited also in these areas due to the morphology of the channel. In contrast the proglacial field immediate to the glacier terminus stream bed friction will have a larger energy input due to the wide shallow channel, additionally radiation will have a greater influence here due to the higher stream surface area and reduced shading (Magnusson *et al.*, 2012).

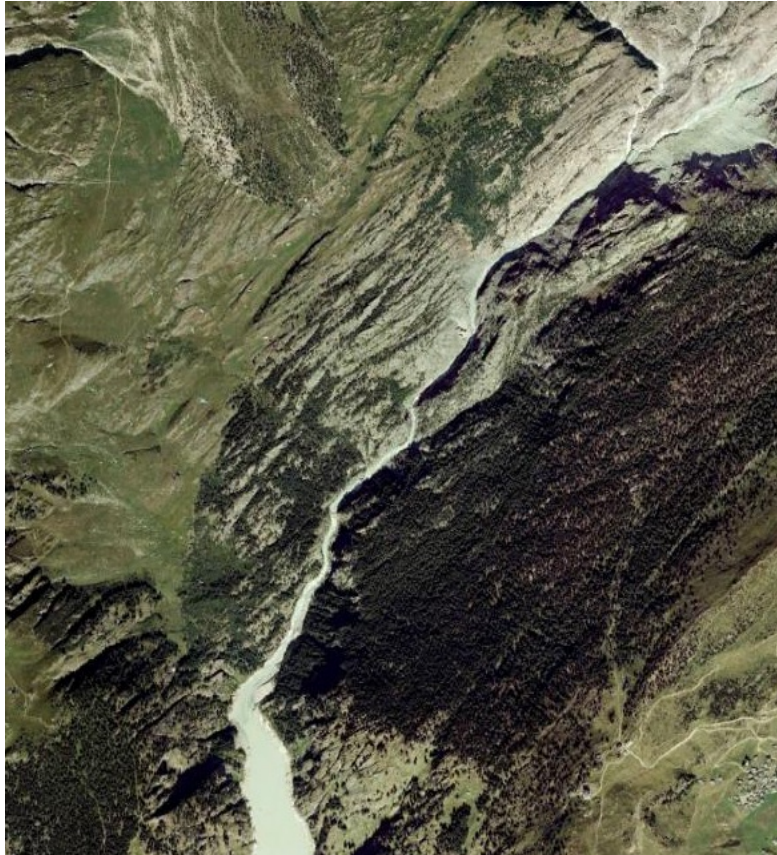


Figure 5.3: Satellite image of the upper reach of Massa demonstrating areas of topographical shading 04/10/2009 (GoogleEarth, 2017).

5.4 Future implications

There has been much debate whether we are currently in a global warming pause; however as Figure 5.4 clearly shows the annual mean temperatures in Switzerland are still increasing. Implications of this are very concerning due to the sensitivity the region has shown with rising transient snowline, less winter snowfall and retreating glaciers. The transient snowline is a major factor when predicting the future regimes of high Alpine hydrology. The elevation of the 0°C isotherm determines whether the catchment receives precipitation in the form of snow or rain, Figure 5.5 displays a schematic diagram of how the vertical movement of the 0°C isotherm determines the area of a basin snow covered or snow free (Collins, 1998). The increasing elevation of the snowline due to global warming is resulting in the basin having

a reduced area covered by snow therefore a lower albedo which in turn increases melt. The higher the previous winter precipitation the lower in elevation the snowline will be, therefore delaying the rise of discharge in the following months. Inevitably the distance between the glacier terminus and gauging station is increasing; therefore the proglacial streams are interacting with the surrounding environment for a longer period of time. The higher residence and transit time increase the amount of time solar radiation has to penetrate the stream, at such a high altitude where UV radiation has significant influence (Brown *et al.*, 2006). This will increase water temperature before it reaches the gauging station. However, bearing in mind that discharge is expected to increase with temperature the volume of water to be heated will result in a decrease water temperature. The relationship between energy input (shortwave radiation), water temperature and discharge can be observed in the schematic diagram shown in Figure 5.6. The findings of the present study are consistent with previous studies on the relationships determining water temperature in a glacier-fed Alpine river (Collins, 2009).

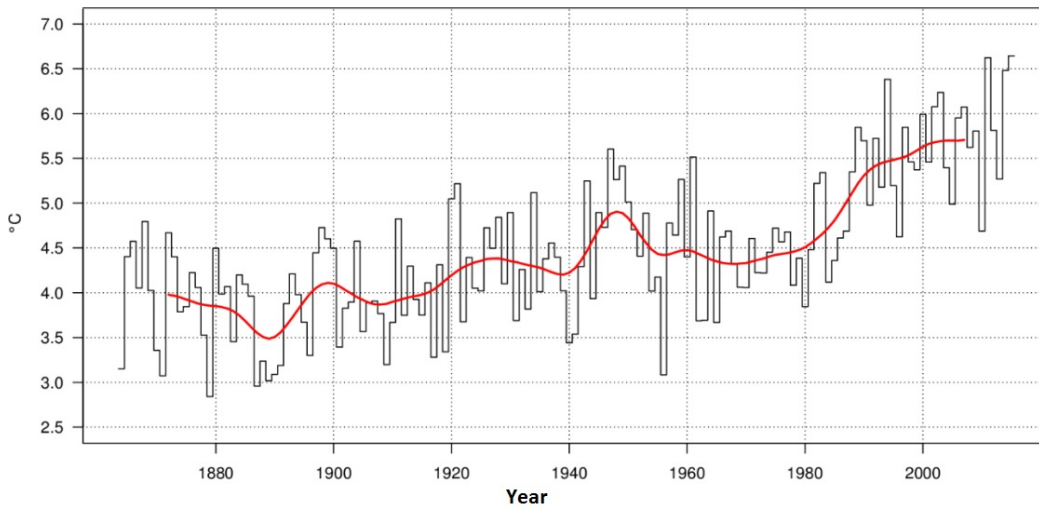


Figure 5.4: Annual mean temperature (°C) in Switzerland from 1864 to 2015. Shown are the mean values of the individual years (black) and the smoothed curve (red) (Meteosuisse, 2016).

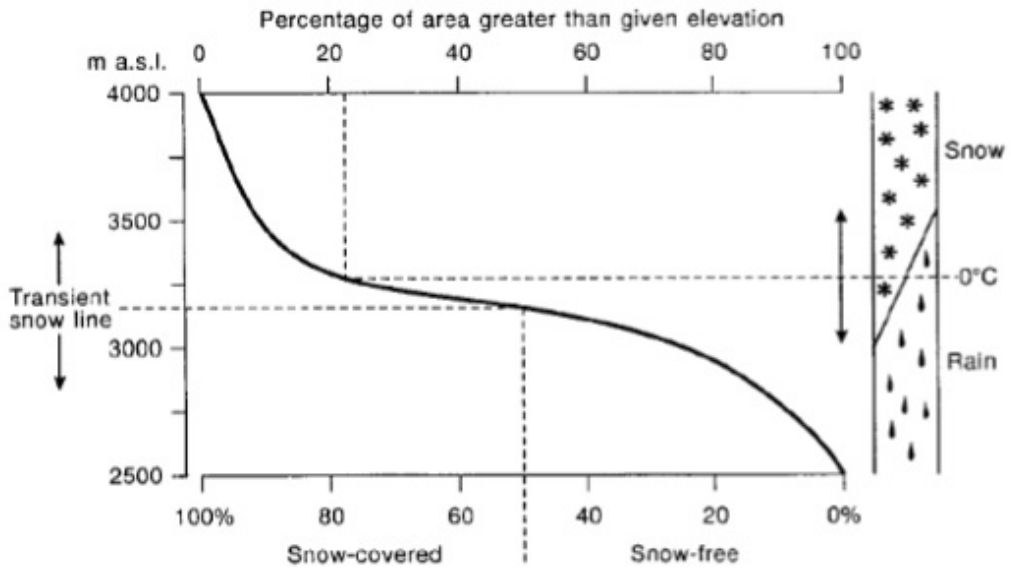


Figure 5.5: Schematic diagram of the transient snowline movement determining the proportion of the basin that receives snowfall or rain (Collins, 1998).

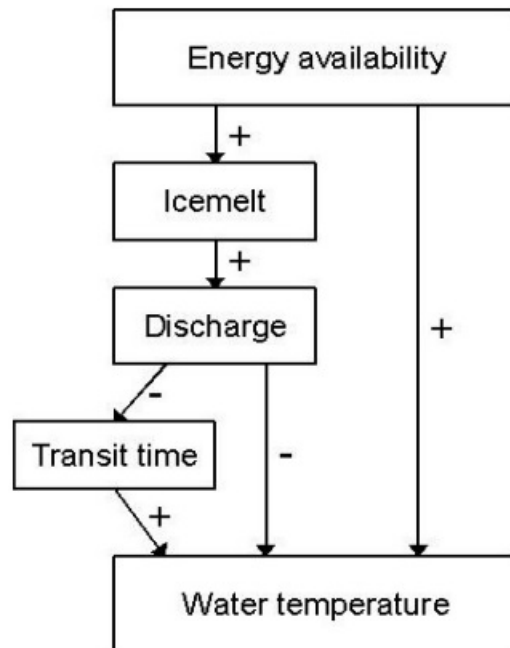


Figure 5.6: Schematic diagram of the relationships between energy input, water temperature and discharge in a river draining from an Alpine glacier (Collins, 2009).

Future implications of continued negative glacier mass balance of Aletschglacier will ultimately result in mean discharge decreasing. Figure 5.7 shows the effect of increasing air temperatures will have on glacier mass and discharge. To begin, discharge will have a negative correlation with glacier mass due to higher levels of icemelt, however as time progresses and mass decreases discharge will hit a tipping point and mean levels will decrease due to less ice available for ablation (Collins *et al.*, 2013). A decrease of discharge will increase the residence time over the proglacial field and reduce the heat capacity of the stream resulting in higher water temperatures. The thermal regime of the Massa will be altered due to groundwater, snow melt and precipitation contributions becoming dominant water sources. Water temperature will therefore reflect air and groundwater temperatures.

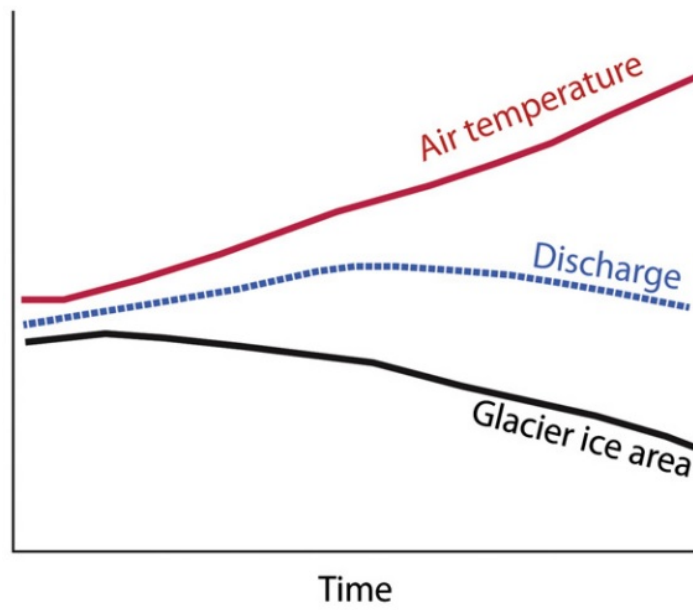


Figure 5.7: Thought experiment to show how temperature increases through time coupled with declining ice area might first increase and then reduce discharge from the ice-covered area of a basin (Collins *et al.*, 2013).

6

Conclusion

The research demonstrates that the relationships between radiation, stream temperature and discharge vary seasonally and demonstrate complexity. Short-wave radiation has the most significant effect on stream temperature in the months January- April; however, once runoff rises from the winter minimum water temperature becomes very much a function of discharge which supports the third hypothesis. A primary objective of the report was to understand why water temperature decreases in spring when radiation remains the same; the results and research support that this occurs in late April and May due to the higher rate of ablation resulting in discharge increasing. Higher runoff increases the heat capacity of the stream as a larger volume and velocity reduces the residence time, therefore less time for radiation to penetrate the stream along with a larger volume of water to be heated resulting in a cooler temperature.

Discharge has an inverse effect on water temperature not only on a seasonal scale but also across annual and diurnal cycles. Periods of high discharge have resulted in cooler water temperatures due to a higher volume of meltwater released from the glacier's terminus at approximately 0 °C. This pattern can be observed annually and diurnally (Figure 4.12). As demonstrated in the results water temperature responds significantly to a small change in discharge, due to the sensitivity to and dependence of proglacial streams on solar radiation as an energy input, where small increases in volume and velocity maximise the heat capacity so that minimal heating occurs. Additionally, stream temperature is sensitive to discharge since during periods of low flow groundwater (higher temperature than meltwater) is a primary source of streams; however once discharge generated from snow and ice melt is added to the system the mean water temperature is reduced. All these

factors contribute to why stream temperature adversely reacts to a small increase of discharge. Another main objective was to identify the level of flow at which a glacier-fed stream's temperature decreases from its peak to the reduced summer levels, for the years 2003-2012 which was $3.54\text{m}^3\text{s}^{-1}$. This has not been highlighted in previous literature. Also the proportion of the annual discharge at which stream temperatures decrease has been determined (Table 4.7).

The final objective of this thesis was the evaluation of the influence radiation has on water temperatures seasonally and diurnally. Proglacial streams have been highlighted to be extremely sensitive to meteorological parameters with radiation a primary energy input (Constantz, 1998; Oerlemans *et al.*, 2009; Sommaruga, 2001). The Massa has reflected this as stream temperature has a strong positive correlation with radiation fluctuations diurnally and in the early ablation period, $r^2=0.82$ demonstrated this close relationship, however in the months May - September when radiation peaks, the Massa does not express this sensitivity as the heat capacity of the stream is high due to increased discharge. The trends on Figure 4.13 highlight the sensitivity proglacial streams have to meteorological forcings as water temperature correlates with radiation with only a 3 hour offset. Therefore water temperature has a positive correlation to radiation and a negative correlation to discharge and the heat capacity of the stream. There has been a consistent relationship between the data sets with peak discharge lagging behind peak water temperature and radiation on a diurnal scale and also seasonal. In addition to this relationship, water temperature and discharge negatively correlate on a diurnal, daily, seasonal and annual scale which signifies discharge been the primary control of stream temperature in glacier-fed rivers.

6.1 Future regimes and further research

Runoff from Alpine glacier-fed rivers like that of the Massa will reflect precipitation in the future as the deglaciation discharge dividend (DDD) continues (Figure 5.7). This therefore will alter the thermal regime of rivers and cause accelerated habitat destruction for species like brown trout due to enhanced water temperature (Hari *et al.*, 2006). Switzerland is highly reliant on seasonal glacier meltwater as a fresh water source and for hydroelectric purposes, therefore the continued observation of Alpine hydrology is key due to the potential decrease of discharge expected when glacier mass hits a tipping point.

Further research to analyse the input of streambed friction and the contribution to runoff meltwater, groundwater and precipitation have is of importance due to the DDD, knowledge of the dominant source will give understanding to future thermal and flow regimes of proglacial streams with meltwater expecting to be less of a significant contributor as glacier mass decreases. Predicting water temperature of proglacial streams draining from a retreating glacier will also be of increasing importance due to the sensitivity proglacial streams have to meteorological parameters, especially with residence time increasing due to the greater distance between the glacier terminus and gauging station.

References

- Barnett, Tim P, Adam, Jennifer C, and Lettenmaier, Dennis P (2005). Potential impacts of a warming climate on water availability in snow-dominated regions. *Nature* **438** (7066), 303–309.
- Battin, Tom J, Wille, Anton, Sattler, Birgit, and Psenner, Roland (2001). Phylogenetic and functional heterogeneity of sediment biofilms along environmental gradients in a glacial stream. *Applied and Environmental Microbiology* **67** (2), 799–807.
- Benyahya, Loubna, Caissie, Daniel, St-Hilaire, André, Ouarda, Taha BMJ, and Bobée, Bernard (2007). A review of statistical water temperature models. *Canadian Water Resources Journal* **32** (3), 179–192.
- Braun, LN and Renner, CB (1992). Application of a conceptual runoff model in different physiographic regions of Switzerland. *Hydrological Sciences Journal* **37** (3), 217–231.
- Brown, GH, Sharp, MJ, Tranter, M, Gurnell, AM, and Nienow, PW (1994). Impact of post-mixing chemical reactions on the major ion chemistry of bulk meltwaters draining the haut glacier d’arolla, valais, Switzerland. *Hydrological Processes* **8** (5), 465–480.
- Brown, Giles H (2002). Glacier meltwater hydrochemistry. *Applied Geochemistry* **17** (7), 855–883.
- Brown, Lee E and Hannah, David M (2008). Spatial heterogeneity of water temperature across an alpine river basin. *Hydrological Processes* **22** (7), 954–967.
- Brown, Lee E, Hannah, David M, and Milner, Alexander M (2006). Thermal variability and stream flow permanency in an alpine river system. *River Research and Applications* **22** (4), 493–501.
- Brown, Lee E, Hannah, David M, and Milner, Alexander M (2007). Vulnerability of alpine stream biodiversity to shrinking glaciers and snowpacks. *Global Change Biology* **13** (5), 958–966.

- Cadbury, SL, Hannah, DM, Milner, AM, Pearson, CP, and Brown, LE (2008). Stream temperature dynamics within a New Zealand glacierized river basin. *River Research and Applications* **24** (1), 68–89.
- Caissie, Daniel (2006). The thermal regime of rivers: a review. *Freshwater Biology* **51** (8), 1389–1406.
- Ceppi, Paulo, Scherrer, Simon C, Fischer, Andreas M, and Appenzeller, Christof (2012). Revisiting Swiss temperature trends 1959–2008. *International Journal of Climatology* **32** (2), 203–213.
- Chikita, Kazuhisa A, Kaminaga, Ryo, Kudo, Isao, Wada, Tomoyuki, and Kim, Yongwon (2010). Parameters determining water temperature of a proglacial stream: the Phelan Creek and the Gulkana Glacier, Alaska. *River research and applications* **26** (8), 995–1004.
- Cogley, J Graham (1979). The albedo of water as a function of latitude. *Monthly Weather Review* **107** (6), 775–781.
- Collins, David N (1984). Climatic variation and runoff from Alpine glaciers. *Zeitschrift für Gletscherkunde und Glazialgeologie* **20**, 127–145.
- Collins, David N (1998). Outburst and rainfall-induced peak runoff events in highly glacierized Alpine basins. *Hydrological processes* **12** (15), 2369–2381.
- Collins, David N (2008). Climatic warming, glacier recession and runoff from Alpine basins after the Little Ice Age maximum. *Annals of Glaciology* **48** (1), 119–124.
- Collins, David N (2009). “Seasonal variations of water temperature and discharge in rivers draining ice-free and partially-glacierised Alpine basins”. In: *Northern Research Basins Symposium*. Vol. 17, 67–74.
- Collins, David N, Davenport, Joshua L, and Stoffel, Markus (2013). Climatic variation and runoff from partially-glacierised Himalayan tributary basins of the Ganges. *Science of the Total Environment* **468**, S48–S59.
- Constantz, Jim (1998). Interaction between stream temperature, streamflow, and groundwater exchanges in alpine streams. *Water resources research* **34** (7), 1609–1615.
- Constantz, Jim, Thomas, Carole L, and Zellweger, Gary (1994). Influence of diurnal variations in stream temperature on streamflow loss and groundwater recharge. *Water resources research* **30** (12), 3253–3264.
- Delpla, I, Jung, A-V, Baures, E, Clement, M, and Thomas, O (2009). Impacts of climate change on surface water quality in relation to drinking water production. *Environment International* **35** (8), 1225–1233.
- Dzikowski, Marc and Jobard, Sylvain (2012). Mixing law versus discharge and electrical conductivity relationships: application to an alpine proglacial stream. *Hydrological Processes* **26** (18), 2724–2732.

- Fenn, CR (1985). Spatial and temporal variations in electrical conductivity in a pro-glacial stream system. *Journal of Glaciology* **31** (108), 108–114.
- Fisher, Stuart G (1995). Stream Ecology: Structure and Function of Running Waters. *Science* **270** (5243), 1858–1859.
- Fountain, Andrew G and Tangborn, Wendell V (1985). The effect of glaciers on streamflow variations. *Water Resources Research* **21** (4), 579–586.
- Gobiet, Andreas, Kotlarski, Sven, Beniston, Martin, Heinrich, Georg, Rajczak, Jan, and Stoffel, Markus (2014). 21st century climate change in the European Alps: a review. *Science of the Total Environment* **493**, 1138–1151.
- Han, Luoheng (1997). Spectral reflectance with varying suspended sediment concentrations in clear and algae-laden waters. *Photogrammetric Engineering and Remote Sensing* **63** (6), 701–705.
- Hari, Renata E, Livingstone, David M, Siber, Rosi, BURKHARDT-HOLM, PATRICIA, and Guettinger, Herbert (2006). Consequences of climatic change for water temperature and brown trout populations in Alpine rivers and streams. *Global Change Biology* **12** (1), 10–26.
- Hill, Margot (2012). *Climate change and water governance: Adaptive capacity in Chile and Switzerland*. Vol. 54. Springer Science & Business Media.
- Huss, Matthias, Farinotti, Daniel, Bauder, Andreas, and Funk, Martin (2008). Modelling runoff from highly glacierized alpine drainage basins in a changing climate. *Hydrological processes* **22** (19), 3888–3902.
- Jouvet, Guillaume, Huss, Matthias, Funk, Martin, and Blatter, Heinz (2011). Modelling the retreat of Grosser Aletschgletscher, Switzerland, in a changing climate. *Journal of Glaciology* **57** (206), 1033–1045.
- Lowney, Cynthia L (2000). Stream temperature variation in regulated rivers: Evidence for a spatial pattern in daily minimum and maximum magnitudes. *Water Resources Research* **36** (10), 2947–2955.
- Magnusson, Jan, Jonas, Tobias, and Kirchner, James W (2012). Temperature dynamics of a proglacial stream: Identifying dominant energy balance components and inferring spatially integrated hydraulic geometry. *Water Resources Research* **48** (6).
- Maizels, Judith K (1979). Proglacial aggradation and changes in braided channel patterns during a period of glacier advance: an Alpine example. *Geografiska Annaler. Series A. Physical Geography*, 87–101.
- Marty, Christoph (2008). Regime shift of snow days in Switzerland. *Geophysical Research Letters* **35** (12).
- Milner, Alexander M, Brown, Lee E, and Hannah, David M (2009). Hydroecological response of river systems to shrinking glaciers. *Hydrological Processes* **23** (1), 62–77.

- Milner, Alexander M and Petts, Geoffrey E (1994). Glacial rivers: physical habitat and ecology. *Freshwater Biology* **32** (2), 295–307.
- Milner, AM, Brittain, JE, Brown, LE, and Hannah, DM (2010). Water sources and habitat of Alpine streams. In: *Alpine Waters*. Springer, 175–191.
- Moore, R Dan, Spittlehouse, DL, and Story, Anthony (2005). RIPARIAN MICROCLIMATE AND STREAM TEMPERATURE RESPONSE TO FOREST HARVESTING: A REVIEW1. *Journal of the American Water Resources Association* **41** (4), 813.
- Oerlemans, J, Giesen, RH, and Van den Broeke, MR (2009). Retreating alpine glaciers: increased melt rates due to accumulation of dust (Vadret da Morteratsch, Switzerland). *Journal of Glaciology* **55** (192), 729–736.
- Poole, Geoffrey C and Berman, Cara H (2001). An ecological perspective on in-stream temperature: natural heat dynamics and mechanisms of human-caused thermal degradation. *Environmental management* **27** (6), 787–802.
- Randin, Christophe F, Engler, Robin, Normand, Signe, Zappa, Massimiliano, Zimmermann, Niklaus E, Pearman, Peter B, Vittoz, Pascal, Thuiller, Wilfried, and Guisan, Antoine (2009). Climate change and plant distribution: local models predict high-elevation persistence. *Global Change Biology* **15** (6), 1557–1569.
- Rebetez, M and Reinhard, M (2008). Monthly air temperature trends in Switzerland 1901–2000 and 1975–2004. *Theoretical and Applied Climatology* **91** (1-4), 27–34.
- Rott, E, Cantonati, M, Füreder, L, and Pfister, P (2006). Benthic algae in high altitude streams of the Alps—a neglected component of the aquatic biota. *Hydrobiologia* **562** (1), 195–216.
- Scherrer, Simon C, Appenzeller, Christof, and Laternser, Martin (2004). Trends in Swiss Alpine snow days: The role of local-and large-scale climate variability. *Geophysical Research Letters* **31** (13).
- Schmucki, Daniel A and Philipona, Rolf (2002). Ultraviolet radiation in the Alps: the altitude effect. *Optical Engineering* **41** (12), 3090–3095.
- Singh, Abhay Kumar and Hasnain, SI (2002). Aspects of weathering and solute acquisition processes controlling chemistry of sub-Alpine proglacial streams of Garhwal Himalaya, India. *Hydrological Processes* **16** (4), 835–849.
- Sommaruga, Ruben (2001). The role of solar UV radiation in the ecology of alpine lakes. *Journal of Photochemistry and Photobiology B: Biology* **62** (1), 35–42.
- Wagnon, Patrick, Ribstein, Pierre, Kaser, Georg, and Berton, Philippe (1999). Energy balance and runoff seasonality of a Bolivian glacier. *Global and planetary change* **22** (1), 49–58.

- Webb, Bruce W, Hannah, David M, Moore, R Dan, Brown, Lee E, and Nobilis, Franz (2008). Recent advances in stream and river temperature research. *Hydrological Processes* **22** (7), 902–918.
- Wegmann, Matthias, Gudmundsson, G Hilmar, and Haeberli, Wilfried (1998). Permafrost changes in rock walls and the retreat of Alpine glaciers: a thermal modelling approach. *Permafrost and Periglacial Processes* **9** (1), 23–33.
- Zemp, Michael, Haeberli, Wilfried, Hoelzle, Martin, and Paul, Frank (2006). Alpine glaciers to disappear within decades? *Geophysical Research Letters* **33** (13).